

Weighted Isolation and Random Cut Forests for Anomaly Detection

Sijin Yeom^{1,2} and Jae-Hun Jung^{1,2,3*}

¹Artificial Intelligence Graduate School, Pohang University of Science and Technology, Pohang, 37673, Korea.

²Mathematical Institute of Data Science, Pohang University of Science and Technology, Pohang, 37673, Korea.

³Department of Mathematics, Pohang University of Science and Technology, Pohang, 37673, Korea.

*Corresponding author(s). E-mail(s): jung153@postech.ac.kr;
Contributing authors: yeomsijin@postech.ac.kr;

Abstract

Random cut forest (RCF) algorithms have been developed for anomaly detection, particularly in time series data. The RCF algorithm is an improved version of the isolation forest (IF) algorithm. Unlike the IF algorithm, the RCF algorithm can determine whether real-time input contains an anomaly by inserting the input into the constructed tree network. Various RCF algorithms, including Robust RCF (RRCF), have been developed, where the cutting procedure is adaptively chosen probabilistically. The RRCF algorithm demonstrates better performance than the IF algorithm, as dimension cuts are decided based on the geometric range of the data, whereas the IF algorithm randomly chooses dimension cuts. However, the overall data structure is not considered in both IF and RRCF, given that split values are chosen randomly. In this paper, we propose new IF and RCF algorithms, referred to as the weighted IF (WIF) and weighted RCF (WRCF) algorithms, respectively. Their split values are determined by considering the density of the given data. To introduce the WIF and WRCF, we first present a new geometric measure, a *density measure*, which is crucial for constructing the WIF and WRCF. We provide various mathematical properties of the density measure, accompanied by theorems that support and validate our claims through numerical examples.

Keywords: Anomaly detection, Isolation forest, Weighted Isolation forest, Robust random cut forest, Weighted random cut forest

1 Introduction

Anomaly detection is a crucial data mining procedure used in various applications such as fraud detection in finance, detection of network intrusion in web infrastructure, etc. [1, 2]. Anomaly detection is a detection algorithm for outliers that deviate from the normal structure of the given data set.

Supervised anomaly detection algorithms use the labeled data, that is, the algorithms are constructed based on the known definition of ‘normal’ and ‘abnormal’ of the data points of the data. In this case, it is straightforward to detect anomalies when the algorithms are well-trained with balanced data sets. Semi-supervised anomaly detection algorithms can also be considered when the labeled samples are limited. However, anomalies are intrinsically rare events, and, in most cases, anomaly samples are rare, thus sometimes it is impossible to label them a priori [3]. Thus the desired anomaly detection algorithms can acquire the notion of anomaly from the data structure without supervision or with semi-supervision.

Such anomaly detection algorithms can be constructed either statistically or geometrically. Recently deep neural network algorithms have been actively developed for anomaly detection [4, 5]. Unlike the neural network approaches, neighbor search approaches such as mining outliers using distance based on the k -th nearest neighbor [6–9] and density-based local outliers [10–12] or the tree approaches such as the isolation forest (IF) [13, 14] and robust random cut forest (RRCF) algorithms [15, 16] are geometric.

The geometric approaches based on the neighbor search using the Euclidean distance are computationally costly. The tree approaches are relatively less costly as they avoid the direct computation of pair-wise distances. The IF and RRCF algorithms partition the given data set forming the binary trees and defining the anomaly score based on the tree. With the ordinary partitioning, however, after choosing a dimension cut, a split value is determined by only two values out of the whole data set. That is, the overall shape of a given data set is not considered.

To consider the overall data structure and improve the existing IF and RRCF algorithms, we introduce a new and improved approach, termed the *Weighted Isolation Forest* (WIF) and the *Weighted Random Cut Forest* (WRCF) algorithms, respectively. In these algorithms, we determine the split values by taking into account the *density* of the data set.

The paper is organized into the following sections. In Sections 2 and 3, we review the IF and RRCF algorithms, respectively. In Section 4, we introduce the density measure and outline its various mathematical characteristics. Section 5 presents our proposed algorithms, namely, the WIF and WRCF. In Section 6, we provide numerical examples demonstrating that the proposed

WIF and WRCF outperform their counterparts, IF and RRCF, especially in scenarios with high data density. The examples aim to illustrate the superior performance of our proposed algorithms. Finally, Section 7 offers a concise concluding remark, summarizing the key findings and contributions of the paper.

2 Isolation Forest

We first explain the isolation forest algorithm introduced in [13]. In this section we formalize mathematical definitions and propositions necessary for the construction of the WIF and WRCF defined in Section 5. The IF algorithm builds a tree by randomly cutting the *bounding boxes* of the data set until all instances are *isolated*. This algorithm doesn't require computing pairwise distances between data points, which can be computationally expensive, especially when the dimension of the data is large.

Given a data set, we create an isolation forest which consists of isolation trees. In an isolation tree, each external *node* of the tree is assigned to an *anomaly score*. The IF algorithm detects anomalies by calculating the anomaly score of each point; the closer the score is to 1, the higher the likelihood of it being an anomaly.

2.1 Binary Trees

When we create a binary tree from data sets in \mathbb{R}^d , we utilize the projection of data sets onto a specific axis. In this case, the projected data sets may contain duplicates. Hence, throughout the paper, we assume that our data set $X \subseteq \mathbb{R}^d$ is a **finite multiset** of $n \geq 2$ elements.

An isolation tree is a *binary tree* constructed in a specific way.

Definition 1 A **binary tree** T of X is a collection of nonempty subsets of X such that

- i) $X \in T$;
- ii) If $D \in T$ with $D \neq X$, then there exists $D' \in T$ such that

$$D \cup D' \in T \text{ and } D \cap D' = \emptyset.$$

- A **subtree** T' in a binary tree T of X is a binary tree of $X' \subseteq X$ such that $T' \subseteq T$.
- An element of T is called a **node** of T .
- The largest node, X , is called the **root node** of T .

Definition 2 A **graph** of a binary tree T is an ordered pair (V, E) such that

- i) $V = T$;
- ii) $E = \{\{D, D_p\} \subseteq V \mid D \subseteq D_p, D_p \setminus D \in V\}$

where V is the set of vertices (or nodes) and E is the set of edges.

Definition 3 Let D, D' and D_p be nodes in a binary tree T where D_p is a disjoint union of D and D' .

- The node D_p is said to be a **parent** node of D and D' .
- The two nodes D and D' are called **children** nodes of D_p .
- We say D' is the **sibling** node of D and vice versa.
- A node that has no children nodes is an **external** (or a **leaf**) node in T .
- A node that is not an external node is an **internal** node in T .
- If every external node of T is a singleton set, then T is said to be **fully grown**.

Definition 4 Let T be a binary tree of X and D be a node in T .

- The **depth** of D , denoted by $d(D, X, T)$, is defined to be the number of edges from D to the root node X in the graph of T .
- We define the **height** of the tree T by the maximum depth of nodes in T , that is,

$$\text{the height of } T = \max\{d(D, X, T) \mid D \in T\}.$$

2.2 Isolation Trees

An isolation tree is obtained from a ‘partitioning process’ which cuts the *bounding boxes* repeatedly. We introduce the basic concept used for the isolation tree, i.e., the partitioning process, and explain how to create an isolation tree through it.

Definition 5 For $q = 1, 2, \dots, d$, we denote the set of the q -th coordinate values in X by

$$X_q = \{x_q \mid (x_1, \dots, x_q, \dots, x_d) \in X\} \subseteq \mathbb{R} \quad (1)$$

which is the projection of X onto the q -th axis. We denote the length of each X_q by

$$l_q = \max X_q - \min X_q. \quad (2)$$

We define the the **bounding box** of X by

$$B(X) = \prod_{q=1}^d [\min X_q, \max X_q]$$

which is the smallest closed cube in \mathbb{R}^d containing X .

Partitioning process for isolation trees.

Step 1. Consider the equally distributed discrete random variable Q of range $\{1, 2, \dots, d\}$ such that:

$$\text{Prob}^{\text{IF}}(Q = q) = \frac{1}{d}$$

for all $q = 1, 2, \dots, d$. Here the chosen $Q = q$ is called the **dimension cut**.

Step 2. Given $Q = q$, we now consider a random value $P|_{Q=q}$ which is uniformly distributed on the closed interval $[\min X_q, \max X_q]$. Here, the chosen $P|_{Q=q} = p$ is called the **split value**.

Step 3. With the dimension cut $q \in \{1, 2, \dots, d\}$ and the split value $p \in [\min X_q, \max X_q]$, we have two outputs

$$\begin{aligned} S_1 &= \{(x_1, \dots, x_q, \dots, x_d) \in X \mid x_q < p\}, \\ S_2 &= \{(x_1, \dots, x_q, \dots, x_d) \in X \mid x_q \geq p\} \end{aligned}$$

where $\{S_1, S_2\}$ is a partition of X .

To build an isolation tree of X , we continue the partitioning process until either

- i) both outputs become singleton sets,
- ii) or, $\min X_q = \max X_q$ for some dimension cut q .

At the end of the partitioning process, a collection of all outputs, including the first input X forms a binary tree called an **isolation tree** of X .

Definition 6 A collection of isolation trees is called an **isolation forest**.

2.3 Anomaly Score

In the IF algorithm, we use the anomaly score $s(x, X, F)$ [13] where x is a point in a data set X and F is an isolation forest. Given a data set X of n elements, the maximum possible height of an isolation tree is $n - 1$ and it grows in the order of n . But the average height of an isolation tree, $c(n)$, is given by

$$c(n) = 2(\ln(n - 1) + \gamma) - \frac{2(n - 1)}{n}$$

which grows in the order of $\ln(n)$ [17] where γ is the Euler–Mascheroni constant:

$$\gamma = \lim_{n \rightarrow \infty} \left(\sum_{k=1}^n \frac{1}{k} - \ln n \right) \approx 0.5772156649.$$

Definition 7 Let F be an isolation forest of X . The anomaly score $s(x, X, F)$ is defined by [13]

$$s(x, X, F) = 2^{-\frac{\mathbb{E}(d(D_x, X, F))}{c(n)}}$$

where D_x is the external node containing x and

$$\mathbb{E}(d(D_x, X, F)) = \frac{1}{|F_x|} \sum_{T \in F_x} d(D_x, X, T)$$

with $F_x = \{T \in F \mid D_x \in T\}$.

Remark 1 [13]

- i) The anomaly score $s(x, X, F)$ is normalized in $(0, 1]$.
- ii) The anomaly score $s(x, X, F)$ is a decreasing function with respect to $d(D_x, X, F)$.
- iii) If $s(x, X, F) \approx 0.5$ for every $x \in X$, then $d(D_x, X, F) \approx c(n)$, that is, the average depth of x in the forest is close to the average height of the isolation trees in the forest. In this case, we may conclude that X has no anomalies.
- iv) If $s(x, X, F)$ is close to 1, then x is regarded as an anomaly.
- v) If $s(x, X, F)$ is less than 0.5, then x is regarded as a normal point.

3 Robust Random Cut Forest

In contrast to the IF, the RRCF consists of *robust random cut trees* (RRCTs) and each external node of a random cut tree has an anomaly score called *collusive displacement*.

3.1 Robust Random Cut Trees

The way of building an RRCT from a data set is the same as the way of building an isolation tree except for the random variable Q . In an isolation tree, a random variable Q has a uniform distribution that only depends on d . In an RRCT, however, a random variable Q depends on the range of each coordinate value of the data set as well as on d .

Partitioning process for RRCTs.

Step 1. Consider the discrete random variable Q of range $\{1, 2, \dots, d\}$ such that

$$\text{Prob}^{\text{RRCF}}(Q = q) = \frac{l_q}{l_1 + \dots + l_d}$$

for $q = 1, 2, \dots, d$. Here the definition of l_q is given in Section 2, specifically in Eq. (2).

Step 2. Given the dimension cut q , we now consider a random value $P|_{Q=q}$ which is uniformly distributed on the closed interval $[\min X_q, \max X_q]$.

Step 3. With the dimension cut $q \in \{1, 2, \dots, d\}$ and the split value $p \in [\min X_q, \max X_q]$, we have a partition of X :

$$\begin{aligned} S_1 &= \{(x_1, \dots, x_q, \dots, x_d) \in X \mid x_q < p\}, \\ S_2 &= \{(x_1, \dots, x_q, \dots, x_d) \in X \mid x_q \geq p\}. \end{aligned}$$

To build a robust random cut tree of X , we continue the partitioning process until both outputs become singleton sets. At the end of the process, a collection of all outputs, including the first input X , forms a binary tree called a **RRCT** of X .

Remark 2

- i) $\text{Prob}^{\text{RRCF}}(Q = q)$ is an increasing function with respect to the length l_q .

- ii) If $\min X_q = \max X_q$ for some q , then $l_q = 0$ and thus $\text{Prob}^{\text{RRCF}}(Q = q) = 0$. Hence we only choose $Q = q$ such that $\min X_q < \max X_q$.
- iii) The partitioning process for RRCTs takes the set X as an input and always gives us two mutually disjoint nonempty subsets S_1, S_2 of X as outputs. In other words, unlike isolation trees, RRCTs are always fully grown.

Definition 8 A collection of RRCTs is called a **robust random cut forest**.

3.2 Anomaly Score

Let T be a robust random cut tree of X . The sum of the depths of all nodes in T

$$|M(T)| = \sum_{D \in T} d(D, X, T)$$

measures how completed the tree T is, so, it is called the **model complexity** of T [15].

The **collusive displacement** of $x \in X$, denoted by $\text{CODISP}(x, X, T)$, is defined to be [15]

$$\max_{x \in D \subsetneq X} \left\{ \frac{1}{|D|} \sum_{y \in X \setminus D} (d(\{y\}, X, T) - d(\{y\}, X \setminus D, T')) \right\}$$

where T' is the tree of $X \setminus D$ such that

$$T' = \{M \setminus D \mid M \in T\}.$$

The graph of T' is obtained by deleting the subtree of D in T and by replacing the parent node D_p of D with the subtree of the sibling node D_s of D (Figs. 1 and 2).

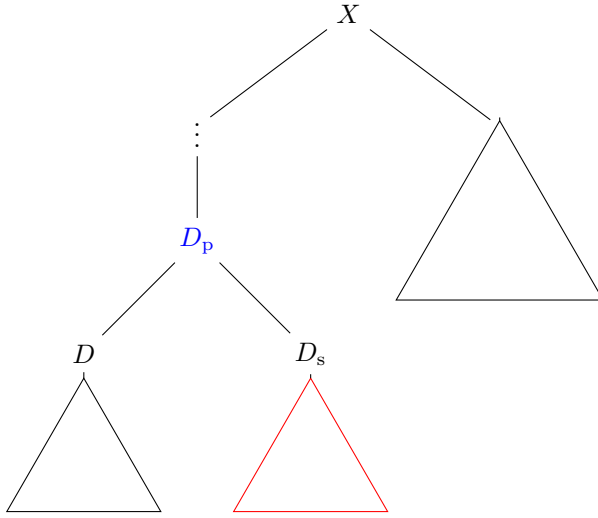
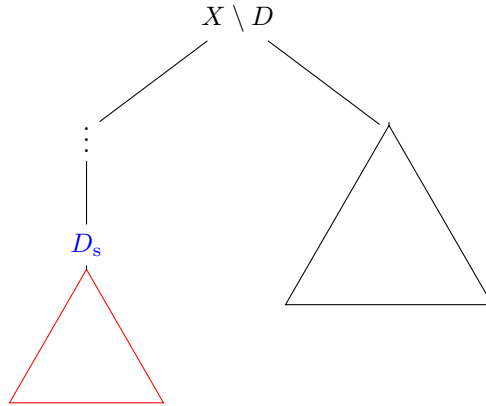
The following Proposition 1 was stated in [15] without proof. Here we provide its proof.

Proposition 1 *Let T be an RRCT of X and D be a node in T with $D \neq X$ and T' be the tree obtained by deleting the subtree of D in T . Then*

$$\sum_{y \in X \setminus D} (d(\{y\}, X, T) - d(\{y\}, X \setminus D, T')) = |D_s|$$

where D_s is the sibling node of D .

Proof Since T is a binary tree and $D \neq X$, D has the parent node D_p and the sibling node D_s . Let T' be the tree of $X \setminus D$ obtained from T deleting the subtree of D . Suppose $y \in X \setminus D$. If $y \notin D_s$, then the number of edges from $\{y\}$ to the root node

**Fig. 1:** The graph of T **Fig. 2:** The graph of T'

X in the tree T and the number of edges from $\{y\}$ to the root node $X \setminus D$ in the tree T' are the same. Thus

$$d(\{y\}, X, T) - d(\{y\}, X \setminus D, T') = 0$$

for each $y \in X \setminus (D \cup D_s)$.

If $y \in D_s$, the number of edges in T from $\{y\}$ to the root node is greater by 1 than those in T' , that is, the edge $\{D_p, D_s\}$ is included in T ;

$$d(\{y\}, X, T) - d(\{y\}, X \setminus D, T') = 1$$

for each $y \in D_s$. Hence we have

$$\begin{aligned}
& \sum_{y \in X \setminus D} (d(\{y\}, X, T) - d(\{y\}, X \setminus D, T')) \\
&= \sum_{y \in D_s} (d(\{y\}, X, T) - d(\{y\}, X \setminus D, T')) \\
&= |D_s|.
\end{aligned}$$

□

Corollary 1 The collusive displacement of $x \in X$ can be calculated effectively by

$$\mathbf{CODISP}(x, X, T) = \max \left\{ \frac{|D_s|}{|D|} \mid x \in D \subsetneq X \right\}.$$

3.3 RRCF with Bagging

The bagging (bootstrap aggregating) is a ‘sampling’ algorithm designed to improve the stability and accuracy of algorithms [18]. We run the RRCF algorithm with bagging by choosing a *sample size* and a *number of iterations*.

Bagging algorithm.

Recall that our data set $X \subseteq \mathbb{R}^d$ is a finite set of n elements.

Step 1. Choose the sample size $s \in \{1, 2, \dots, n\}$ and the number of iterations $N \in \mathbb{N}$. Let k be the greatest integer less than or equal to $\frac{n}{s}$, that is, $k = \lfloor \frac{n}{s} \rfloor$. Let j be the number of repetitions of **Step 2**.

Step 2. We construct k samples $S_{1,j}, \dots, S_{k,j}$ where each $S_{1,j}$ consists of s points, randomly chosen from X . Apply the RRCF algorithm to $S_{1,j}, \dots, S_{k,j}$. For each sample $S_{i,j}$, we obtain an RRCT, $T_{i,j}$ and $\mathbf{CODISP}(x, S_{i,j}, T_{i,j})$ for each $x \in T_{i,j}$.

Step 3. Repeat **Step 2** N times and obtain an RRCF, F_j

$$F_j = \{T_{1,j}, T_{2,j}, \dots, T_{k,j}\}$$

for $j = 1, 2, \dots, N$. Then we have the **average collusive displacement** of $x \in X$,

$$\mathbf{Avg-CODISP}(x, N) = \frac{1}{a(x)} \sum_{j=1}^N \sum_{T_{i,j} \in F_j} \mathbf{CODISP}(x, S_{i,j}, T_{i,j})$$

where

$$a(x) = \sum_{j=1}^N \sum_{T_{i,j} \in F_j} |\{x\} \cap S_{i,j}|$$

is the number of times x appears in the bagging algorithm. In most cases, the RRCF algorithm is employed with bagging.

3.4 RRCF for time series data

Given an RRCT T of a data set X , we can construct a new tree T' by deleting a point from X or inserting a new point to X . In this way, one can apply the RRCF algorithm to time series data effectively.

3.4.1 Deleting a point from a tree

Let T be an RRCT of a data set $X \subseteq \mathbb{R}^d$ and let $x \in X$. The tree T' obtained by deleting the point x is defined by

$$T' = \{D \setminus \{x\} \mid D \in T\}.$$

The graph of T' can be visualized by deleting the node of $\{x\}$ in T and by replacing the parents node D_p of $\{x\}$ with the subtree of the sibling node D_s of D (Figs. 3 and 4).

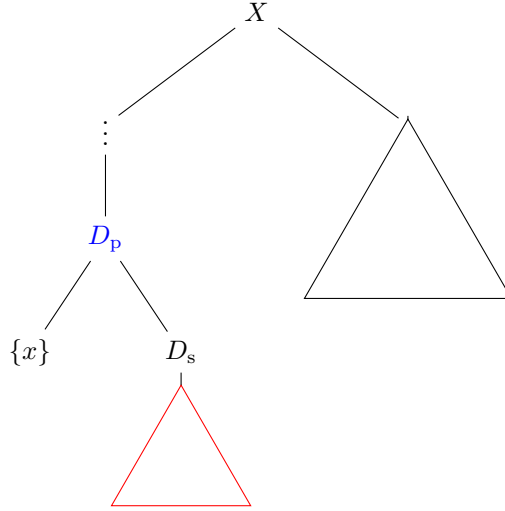


Fig. 3: The graph of T

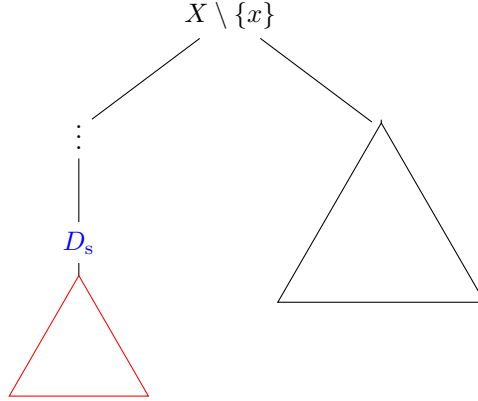
3.4.2 Inserting a point to a tree

Let T be an RRCT of a data set $X \subseteq \mathbb{R}^d$. Let $y \in \mathbb{R}^d \setminus X$ be a new point.

Building process of a tree with a new point.

Step 1. Consider the bounding box of $X' = X \cup \{y\}$

$$B(X') = \prod_{q=1}^d [\min X'_q, \max X'_q]$$

**Fig. 4:** The graph of T'

and the total length l' of ‘edges’ of the box

$$l' = \sum_{q=1}^d (\max X'_q - \min X'_q).$$

Step 2. Let R be a random variable that is uniformly distributed on $[0, l']$. Choose $r \in [0, l']$ from the random variable R and obtain the values s and c :

$$s = \operatorname{argmin} \left\{ t \in \{1, 2, \dots, d\} \mid \sum_{i=1}^t (\max X_i - \min X_i) \geq r \right\},$$

$$c = \min X'_q + r - \sum_{i=1}^{s-1} (\max X'_i - \min X'_i).$$

Step 3. There are two cases:

Case 1. $c \notin [\min X_s, \max X_s]$ (Fig. 5).

In this case, X' has a fully grown binary tree $T' = \{X', T, \{y\}\}$ of X' .

Case 2. $c \in [\min X_s, \max X_s]$ (Fig. 6).

Choose the same dimension cut s and the split value p in the partitioning process for T used to partition $X = X' \setminus \{y\}$ and apply the partition process for RRCTs to X' with the values of s, p . Then we have a binary tree $T' = \{X', A, B\}$ where $y \in A$ and $A \cup B = X'$. Note that B is also a node in T whose parent is X . We update the binary tree T' by replacing the node B with the subtree T_B of B in T (Fig. 7).

To build an RRCT T' of X' , apply this process repeatedly to the output A in **Case 2** of **Step 3** by replacing X' with A in **Step 1** and by replacing X with $A \setminus \{y\}$ in **Step 3** until $\{y\}$ becomes an external node.

Remark 3

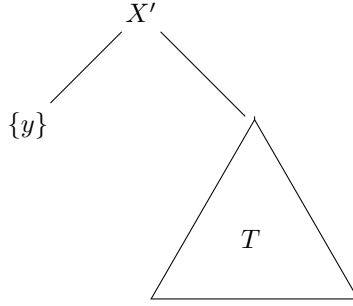


Fig. 5: The graph of T' when $c \notin [\min X_s, \max X_s]$

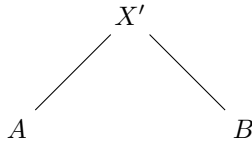


Fig. 6: The graph of $T' = \{X', A, B\}$

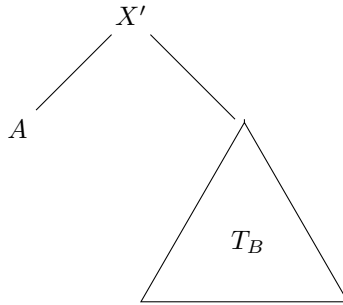


Fig. 7: The graph of $T' = \{X', A\} \cup T_B$

- i) If **Case 1** of **Step 3** holds, $\{y\}$ becomes an external node.
- ii) In **Case 2** of **Step 3**, the node A containing y has less elements than X' and thus the process terminates and $\{y\}$ must become an external node in finite time.

3.4.3 Application to time series data

A time series data $X = \{x_t\}_{t=1}^n \subseteq \mathbb{R}$ is a finite sequence with respect to time t . To apply the RRCF algorithm to the time series data X , we use the sliding window technique [19] and set shingle size = h , window size = w , and forest size = r .

The following steps show the detailed procedure of how to apply the RRCF algorithm to time series data.

Step 1. We make a new data set S which can be obtained from X by constructing *shingles* and apply the RRCF algorithm to the new set S : Choose a **shingle size** $1 \leq h \leq n$ and obtain $n - h + 1$ **shingles** $s_t \in \mathbb{R}^h$ defined by

$$\begin{aligned} s_1 &= (x_1, x_2, \dots, x_h), \\ s_2 &= (x_2, x_3, \dots, x_{h+1}), \\ &\vdots \\ s_{n-h+1} &= (x_{n-h+1}, x_{n-h+2}, \dots, x_n). \end{aligned}$$

Instead of X , we apply the RRCF algorithm with bagging to

$$S = \{s_t \in \mathbb{R}^h \mid t = 1, 2, \dots, n - h + 1\}.$$

Step 2. Choose a **window size** w and a forest size r . Let $n' = n - h + 1$ be the number of elements in S . For $i = 1, 2, \dots, n' - w + 1$, we have a **window**

$$W_i = \{s_i, s_{i+1}, \dots, s_{i+w-1}\} \subseteq S.$$

Construct an RRCF F_1 which has r RRCTs of W_1 . For each RRCT $T \in F_i$ with $i \geq 1$, we obtain a ‘next’ RRCT $T' \in F_{i+1}$ in the following way:

- i) Delete a point s_i from $T \in F_i$ and get the tree T'' .
- ii) Insert a point s_{i+w} to the tree T'' and get a tree T' of W_{i+1} .

Then we have the **collusive displacement** of s_j [15] given by

$$\begin{cases} \frac{1}{j} \sum_{i=1}^j \left(\frac{1}{r} \sum_{T \in F_i} \mathbf{CODISP}(s_j, W_i, T) \right) & \text{if } 1 \leq j \leq w, \\ \frac{1}{w} \sum_{i=j-w+1}^j \left(\frac{1}{r} \sum_{T \in F_i} \mathbf{CODISP}(s_j, W_i, T) \right) & \text{if } w < j \leq n' - w, \\ \frac{1}{n'-j+1} \sum_{i=j-w+1}^{n'-w+1} \left(\frac{1}{r} \sum_{T \in F_i} \mathbf{CODISP}(s_j, W_i, T) \right) & \text{if } n' - w < j \leq n'. \end{cases}$$

When we apply the RRCF algorithm to time series data, we will write $\mathbf{CODISP}(x)$ denoting $\mathbf{Avg-CODISP}(x)$.

Remark 4

- i) To obtain the **Avg-CODISP** of s_j , we calculate every **CODISP** of s_j over all windows which contain s_j .
- ii) Suppose we have a new point x_{n+1} . Put $s_{n'+1} = s_{n-m} = (x_{n-m}, \dots, x_{n+1})$. Then we have the new window

$$W_{n'-w+2} = \{s_{n'-w+2}, s_{n'-w+3}, \dots, s_{n'+1}\} \subseteq S \cup \{s_{n'+1}\}.$$

	IF	RRCF
Dimension Cuts	$\text{Prob}^{\text{IF}}(Q = q) = \frac{1}{d}$	$\text{Prob}^{\text{RRCF}}(Q = q) = \frac{l_q}{l}$
Split Values	randomly chosen in $[m, M]$	

Table 1: The method for determining dimension cuts and split values in the IF and RRCF algorithms

We construct an RRCF F_{n+1} in the same way and have

$$\text{Avg-CODISP}(s_{n+1}) = \frac{1}{r} \sum_{T \in F_{n'-w+2}} \text{CODISP}(s_j, W_{n-w+2}, T).$$

4 Density Measure

To introduce our proposed WIF (weightd IF) and WRCF (weighted RCF) in Section 5, we begin by introducing the density measure. We first address the motivation behind the density measure through an example, illustrating certain issues with ordinary partitioning (referenced in Section 4.1). Following that, we formally define the density measure in Section 4.2. In Section 4.3, we will demonstrate that the density measure we define is invariant under scaling and translation and possesses the property that its values approach 1 when the data is denser than a uniform distribution and approach 0 when the data is sparser than or close to a uniform distribution.

4.1 Motivation

For an isolation tree or an RRCT from a given data set X , we have used the split value p , obtained from the random variable

$$P|_{Q=q} \sim \text{Uniform}[m, M]$$

where q is a dimension cut and $m = \min X_q$, $M = \max X_q$. Note that the random variable $P|_{Q=q}$ is determined by only two values m and M . Both the IF and RRCF algorithms do not take the given data structure into account when choosing the split values.

In Table 1, we see that the RRCF uses improved dimension cuts but it still uses the same method as the IF algorithm when determining the split values. Example 1 illustrates this particular issue.

Example 1 Consider a set $X \subseteq \mathbb{R}^2$ of 6 points given by

$$X = \{(0, 0), (1, 0), (2, 0), (10, 0), (11, 0), (12, 0)\}.$$

Note that the y -coordinate values of X are all zero, that is, $\min X_2 = \max X_2 = 0$. Therefore, $\text{Prob}(Q = 2) = 0$ and so we only consider $P|_{Q=1}$. Considering the ‘shape’ of X , one might think there are two clusters

$$S_1 = \{(0, 0), (1, 0), (2, 0)\},$$

$$S_2 = \{(10, 0), (11, 0), (12, 0)\}$$

and want to have the binary tree $T = \{X, S_1, S_2\}$ as in Fig. 8.

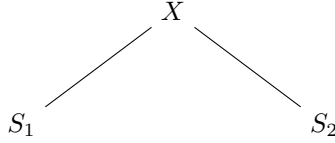


Fig. 8: The desired graph of T (Example 1)

Having the tree T in Fig. 8 is equivalent to using the split value $p \in (2, 10)$. But if we choose the split value p obtained from the random variable $P|_{Q=1}$, which is uniformly distributed on $[0, 12]$, we have

$$\text{Prob}(2 < P|_{Q=1} < 10) = \frac{8}{12} = \frac{2}{3}$$

which is the probability of building the tree T in Fig. 8 at the first partitioning process. In other words, we would miss the tree with the probability of $\frac{1}{3}$.

4.2 Definitions

As seen in Example 1, the ordinary partitioning algorithm does not consider the shape of X . To address this limitation and take into account the shape of the data, we introduce a new partitioning algorithm called *Density-Aware Partitioning* (Section 5.1). This algorithm is designed to overcome the mentioned issue. Before introducing the new method, we define a density measure μ that quantifies the ‘density’ of the given data set X .

Definition 9 Let F_0 be the collection of all nonempty finite sets in \mathbb{R} . For each $Y \in F_0$, we define the radius of Y by

$$\varepsilon = \begin{cases} \frac{\max Y - \min Y}{2(|Y|-1)} & \text{if } |Y| \neq 1, \\ 0 & \text{if } |Y| = 1. \end{cases}$$

Denote the half-open interval of radius ε centered at p by

$$I_{p,\varepsilon} = \begin{cases} [p - \varepsilon, p + \varepsilon) & \text{if } \varepsilon > 0, \\ \{p\} & \text{if } \varepsilon = 0. \end{cases}$$

The **density measure** μ_0 on \mathbb{R} is a map defined by

$$\mu_0 : F_0 \rightarrow [0, 1]$$

$$Y \mapsto \max \left\{ \frac{|I_{p,\varepsilon} \cap Y|}{|Y|} \mid p \in [\min Y, \max Y] \right\}.$$

Definition 10 Let F be the collection of all nonempty finite sets in \mathbb{R}^d . The **density measure** μ on \mathbb{R}^d is a map defined by

$$\mu : F \rightarrow [0, 1]$$

$$X \mapsto \frac{1}{d} \sum_{q=1}^d \mu_0(X_q).$$

The definition of X_q is provided in Section 2, specifically in Eq. (1).

Remark 5

If $Y = \{a, 2a, \dots, na\}$, which is equally distributed with distance $a > 0$, then

$$\varepsilon = \frac{an - a}{2(n-1)} = \frac{a}{2}.$$

Thus the radius of Y is the half of the equal distance a and $[p - \frac{1}{2}a, p + \frac{1}{2}a) \cap Y$ has only one element for all $p \in [a, na]$. Thus we have

$$\begin{aligned} \mu(Y) &= \max \left\{ \frac{|[p - \frac{1}{2}a, p + \frac{1}{2}a) \cap Y|}{n} \mid p \in [a, na] \right\} \\ &= \frac{1}{n}. \end{aligned}$$

Example 2 illustrates the density measure for the 2D-defined data with some examples.

Example 2 Let C_0 and C_2 be sets of 50 and 5 points in \mathbb{R}^2 respectively, where each point of both sets is obtained from the random variable (A, B) such that both A and B are normally distributed. For each $k > 0$, define

$$C_1 = \left\{ \frac{1}{k}(x, y) \mid (x, y) \in C_0 \right\}.$$

Put $X = C_1 \cup C_2$. For each $k = 1, 5, 30$ and 50 , the densities of X are depicted in Fig. 9. As shown in the figure, an increase in sparsity results in a decrease in the density measure. Note that X with $k = 5, 30$ and 50 have all the same bounding box and so the IF and RRCF would treat them equally when choosing the split values at the first partitioning step.

4.3 Propositions

We investigate the properties of the proposed density measure. Propositions 2 and 3 examine two extreme cases of X_q with respect to the density measure μ . Propositions 4 and 5 demonstrate that the density measure is invariant under reflection, scaling, and translation.

Proposition 2 Fix $q \in \{1, 2, \dots, d\}$. The following statements are equivalent:

- i) X_q is uniformly distributed, that is, $X_q = \{ak + b \mid k = 1, 2, \dots, n\}$ for some $a > 0, b \in \mathbb{R}$.
- ii) $\mu(X_q) = \frac{1}{n}$ where n is the number of elements in X_q .

Proof Let $m = \min X_q$ and $M = \max X_q$.

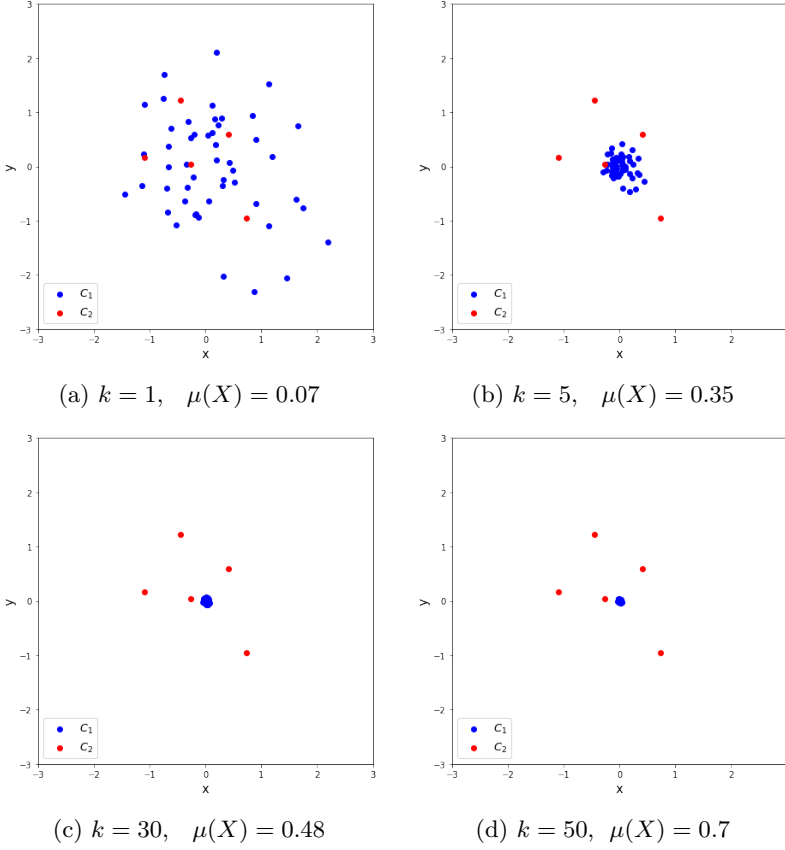


Fig. 9: The graph of $X = C_1 \cup C_2$ (Example 2)

1) i) \Rightarrow ii): Suppose that i) holds. Then we have

$$\varepsilon_q = \frac{M - m}{2(n - 1)} = \frac{a(n - 1)}{2(n - 1)} = \frac{a}{2}$$

and therefore

$$I_{p, \varepsilon_q} = \left[p - \frac{a}{2}, p + \frac{a}{2} \right).$$

If we write $x_k = ak + b$ for $k = 1, 2, \dots, n$, then

$$x_{k+1} - x_k = a$$

for $k \in \{1, 2, \dots, n - 1\}$. For any $p \in [x_k, x_{k+1})$ with $k \in \{1, 2, \dots, n - 1\}$,

$$I_{p, \varepsilon_q} \cap X_q = \left[p - \frac{a}{2}, p + \frac{a}{2} \right) \cap X_q = \{x_k\}$$

which shows $|I_{p, \varepsilon_q} \cap X_q| = 1$ for all $p \in [m, M]$. Thus we have

$$\mu(X_q) = \max \left\{ \frac{|I_{p, \varepsilon_q} \cap X_q|}{n} \mid p \in [m, M] \right\} = \frac{1}{n}.$$

- 2) ii) \Rightarrow i): Suppose $\mu(X_q) = \frac{1}{n}$. Then $|I_{p,\varepsilon_q} \cap X_q| = 1$ for all $p \in [m, M]$. Write $X = \{x_1, \dots, x_n\}$ with $x_1 \leq x_2 \leq \dots \leq x_n$. Then we must have

$$x_k = x_1 + \varepsilon_q(k-1)$$

for $k = 1, 2, \dots, n-1$. This proves i) by taking $a = \varepsilon_q > 0$ and $b = x_1 - \varepsilon_q$. \square

Note that Proposition 2 is the generalization of Remark 5.

Proposition 3 Fix $q \in \{1, 2, \dots, d\}$. The following statements are equivalent:

- i) X_q is a multiset where all the elements are identical.
- ii) $\mu(X_q) = 1$.

Proof Let $m = \min X_q$ and $M = \max X_q$.

- 1) i) \Rightarrow ii): Suppose that $X_q = \{x, \dots, x\}$ with n duplicates. Since $m = x = M$, we have $\varepsilon_q = 0$ and $I_{p,0} = \{x\} = X_q$. Then

$$\begin{aligned} \mu(X) &= \frac{1}{d} \sum_{q=1}^d \max \left\{ \frac{|I_{p,\varepsilon_q} \cap X_q|}{n} \mid p \in [m, M] \right\} \\ &= \frac{1}{d} \sum_{q=1}^d \max \left\{ \frac{|X_q \cap X_q|}{n} \right\} \\ &= \frac{1}{d} \sum_{q=1}^d \max \left\{ \frac{n}{n} \right\} \\ &= 1. \end{aligned}$$

- 2) ii) \Rightarrow i): Suppose $\mu(X_q) = 1$. Clearly, i) holds for $n = 1$. Assume that $n \geq 2$. Since $\mu(X_q) = 1$, we must have

$$\max \left\{ \frac{|I_{p,\varepsilon_q} \cap X_q|}{n} \mid p \in [m, M] \right\} = 1.$$

Then there exist $p_0 \in [m, M]$ such that $|I_{p_0,\varepsilon_q} \cap X_q| = n$, that is, $X_q \subseteq I_{p_0,\varepsilon_q}$. Suppose $m < M$. Then

$$I_{p_0,\varepsilon_q} = \left[p_0 - \frac{M-m}{2(n-1)}, p_0 + \frac{M-m}{2(n-1)} \right)$$

must contain both m and M and thus

$$p_0 - \frac{M-m}{2(n-1)} \leq m < M < p_0 + \frac{M-m}{2(n-1)}.$$

Then we have

$$\frac{(2n-3)M+m}{2(n-1)} < p_0 \leq \frac{M+(2n-3)m}{2(n-1)}.$$

By comparing the left and right sides of the above inequality, we have

$$\begin{aligned} \frac{(2n-3)M+m}{2(n-1)} &< \frac{M+(2n-3)m}{2(n-1)} \\ \Leftrightarrow (2n-3)M+m &< M+(2n-3)m \\ \Leftrightarrow (2n-4)M &< (2n-4)m. \\ \Leftrightarrow M &\leq m. \end{aligned}$$

Hence, we must have $m = M$, that is, all the elements of X_q are identical. Therefore, we have $X_q = \{p_0, \dots, p_0\}$ with n duplicates. \square

Proposition 4 *The density measure μ is invariant with respect to reflection, that is,*

$$\mu(X) = \mu(-X).$$

Proof Fix $q \in \{1, 2, \dots, d\}$. Clearly, we have

$$\varepsilon_{q,X} = \frac{-\min X_q - (-\max X_q)}{2n-1} = \varepsilon_{q,(-X)}.$$

Let $p_0 \in [\min X_q, \max X_q]$ such that $\mu_0(X_q) = \frac{|I_{p_0, \varepsilon_{q,X}} \cap X_q|}{|X_q|}$. Write $I_{p_0, \varepsilon_{q,X}} \cap X_q = \{a_1, a_2, \dots, a_k\}$. Then we have

$$\begin{aligned} \mu_0(X_q) &= \frac{|\{a_1, a_2, \dots, a_k\}|}{|X_q|} \\ &= \frac{|\{-a_1, -a_2, \dots, -a_k\}|}{|(-X)_q|} \\ &= \mu_0((-X)_q) \end{aligned}$$

where $q \in \{1, \dots, d\}$ can be arbitrary. Hence, $\mu(X) = \mu(-X)$. \square

Proposition 5 *The density measure μ is invariant with respect to scaling and translation. That is,*

$$\mu(X) = \mu(aX + b)$$

for any $a \neq 0, b \in \mathbb{R}$.

Proof Fix $q \in \{1, 2, \dots, d\}$. If X_q has n duplicates, then $aX_q + b$ also has n duplicates. By **Proposition 3**, we have

$$\mu_0(X_q) = 1 = \mu_0(aX_q + b).$$

By **Proposition 4**, $\mu_0(aX_q) = \mu_0(-aX_q)$ and so we may assume that $a > 0$. Suppose that $\min X_q < \max X_q$ and let

$$Y_q = aX_q + b = \{ax + b \mid x \in X_q\}.$$

Then we have

$$\begin{aligned} \varepsilon_{q,Y} &= \frac{(a \max X_q + b) - (a \min X_q + b)}{2(n-1)} \\ &= a\varepsilon_{q,X} \end{aligned}$$

and

$$\begin{aligned} &x \in I_{p, \varepsilon_{p,X}} \cap X_q \\ \Leftrightarrow &x \in [p - \varepsilon_{q,X}, p + \varepsilon_{q,X}) \cap X_q \\ \Leftrightarrow &ax + b \in [a(p - \varepsilon_{q,X}) + b, a(p + \varepsilon_{q,X}) + b) \cap (aX_q + b) \\ \Leftrightarrow &y \in [p' - \varepsilon_{q,Y}, p' + \varepsilon_{q,Y}) \cap Y_q \text{ with } p' = ap + b \\ \Leftrightarrow &y \in I_{p', \varepsilon_{q,Y}} \cap Y_q. \end{aligned}$$

Therefore,

$$\begin{aligned}\mu_0(X_q) &= \max \left\{ \frac{|I_{p, \varepsilon_q, X} \cap X_q|}{n} \mid p \in [\min X_q, \max X_q] \right\} \\ &= \max \left\{ \frac{|I_{p', \varepsilon_q, Y} \cap Y_q|}{n} \mid p' \in [\min Y_q, \max Y_q] \right\} \\ &= \mu_0(Y_q)\end{aligned}$$

where $q \in \{1, \dots, d\}$ can be arbitrary. Hence, $\mu(X) = \mu(aX + b)$. \square

5 Weighted Isolation Forest and Weighted Random Cut Forest

A *Weighted Isolation Forest* (WIF) and a *Weighted Random Cut Forest* (WRCF) are similar to the IF and RRCF, respectively. The key distinction lies in how the new algorithms, WIF and WRCF, select the split value p through *density-aware partitioning*. The goal of density-aware partitioning is to avoid ‘bad’ split values located in a cluster in the data set.

5.1 Density-Aware Partitioning

Suppose that the dimension cut $q \in \{1, 2, \dots, d\}$ is chosen. Choose an integer $\alpha \geq 2$.

Stage 1. Choose the split value p as usual from the random variable

$$P|_{Q=q} \sim \text{Uniform}[\min X_q, \max X_q].$$

Stage 2. If $|I_{p, \varepsilon_q} \cap X_q| \geq \alpha$, we repeat **Stage 1** until we choose p such that

$$|I_{p, \varepsilon_q} \cap X_q| < \alpha.$$

Remark 6

- i) A split value p with $|I_{p, \varepsilon_q} \cap X_q| \geq \alpha$ is regarded as being in a cluster.
- ii) The probability that the partitioning process does not terminate within n trials is

$$(\text{Prob}(|I_{P|_{Q=q, \varepsilon_q}} \cap X_q| \geq \alpha))^n.$$

We will show later in **Theorem 7** that this probability is highly small and we do not have to worry about the infinite loop in **Stage 2**.

Recall Example 1 in **Section 4.1**. In this case, X has high density with $\mu(X) = 0.75$. We will build a binary tree with the new process of choosing the split value p . Note that

$$\varepsilon_1 = \frac{12 - 0}{2(6 - 1)} = 1.2.$$

Define a map f as

$$\begin{aligned} f : [0, 12] &\rightarrow \mathbb{Z} \\ p &\mapsto |I_{p, \varepsilon_1} \cap X_1|. \end{aligned}$$

Then we have

$$f(p) = |I_{p, \varepsilon_1} \cap X_1| = \begin{cases} 2 & \text{if } 0 \leq p \leq 0.8 \\ 3 & \text{if } 0.8 < p \leq 1.2 \\ 2 & \text{if } 1.2 < p \leq 2.2 \\ 1 & \text{if } 2.2 < p \leq 3.2 \\ 0 & \text{if } 3.2 \leq p < 8.8 \\ 1 & \text{if } 8.8 \leq p \leq 9.8 \\ 2 & \text{if } 9.8 < p \leq 10.8 \\ 3 & \text{if } 10.8 < p \leq 11.2 \\ 2 & \text{if } 11.2 < p \leq 12 \end{cases}$$

with the graph shown in Fig. 10.

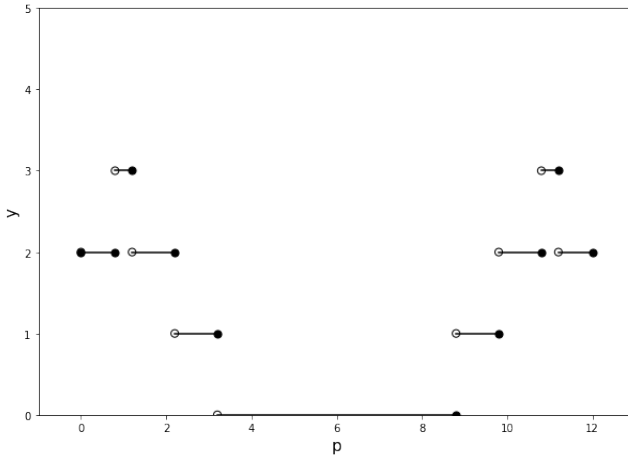
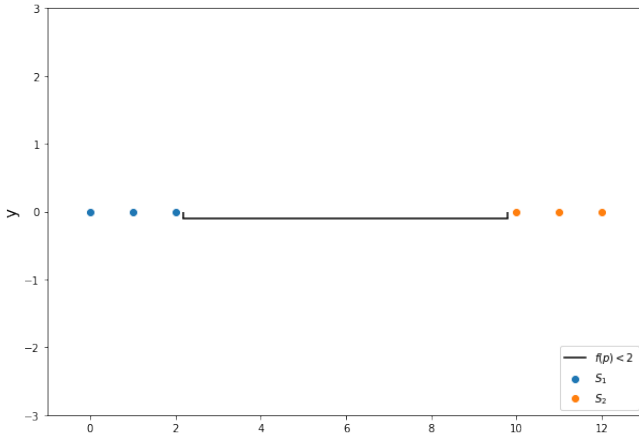


Fig. 10: The graph of $y = f(p)$

If we take $\alpha > 3$, we always have $|I_{p, \varepsilon_1} \cap X_1| < \alpha$ and thus we never repeat **Stage 1**. Suppose $\alpha = 2$ and note that

$$f(p) = |I_{p, \varepsilon_1} \cap X_1| < 2 \Leftrightarrow 2.2 < p \leq 9.8.$$

Figure 11 illustrates the case with the six points from Example 1. The extended solid line represents the interval where $f(p) < 2$. We *always* have the binary

**Fig. 11:** The graph of points in X (Example 1)

N	1	2	3	4	5
$1 - \left(\frac{11}{30}\right)^N$	0.63	0.87	0.95	0.98	0.99

Table 2: The probability that the new process terminates within $N - 1$ trials

tree $T = \{X, S_1, S_2\}$ (Fig. 8) with the density-aware partitioning ($\alpha = 2$). The probability that we repeat **Stage 1** is

$$\frac{\mu_{\text{Bor}}(A)}{\mu_{\text{Bor}}([0, 12])} = \frac{(2.2 - 0) + (12 - 9.8)}{12 - 0} = \frac{11}{30}$$

where μ_{Bor} is the Borel measure [20] on \mathbb{R} and $A = \{p \in [0, 12] : f(p) \geq 2\}$. Hence, the probability that we repeat **Stage 1** N times is $\left(\frac{11}{30}\right)^N$. In other words, the probability that the new process terminates within $N - 1$ trials is $1 - \left(\frac{11}{30}\right)^N$. In Table 2, we find that the new process terminates within 3 trials with the probability of 98.2%. In Section 5.3, we will show that this probability has a lower bound (Table 3).

5.2 WIF and WRCF

Recall that the IF and RRCF use an ordinary partitioning process (Algorithm 1) where split values are determined without considering the shape or density of the data. The WIF and WRCF are obtained by choosing split values with density-aware partitioning (Algorithm 2). This enhancement allows our proposed algorithms to take into account the shape and density of the data set.

Algorithm 1 Ordinary Partitioning

-
- 1: Suppose dimension cut $q \in \{1, 2, \dots, d\}$ is chosen.
 - 2: Choose split value p from $P|_{Q=q} \sim \text{Uniform}[\min X_q, \max X_q]$.
-

Algorithm 2 Density-Aware Partitioning

-
- 1: Suppose dimension cut $q \in \{1, 2, \dots, d\}$ is chosen.
 - 2: Choose an integer $\alpha \geq 2$.
 - 3: **procedure** STAGE 1
 - 4: Choose split value p from $P|_{Q=q} \sim \text{Uniform}[\min X_q, \max X_q]$.
 - 5: **end procedure**
 - 6: **procedure** STAGE 2
 - 7: **while** $|I_{p, \varepsilon_q} \cap X_q| \geq \alpha$ **do**
 - 8: **do** Stage 1
 - 9: **end while**
 - 10: **end procedure**
-

5.3 Proposition and Theorem

Proposition 6 demonstrates the existence of the split value p , while Theorem 7 establishes that the density-aware partitioning eventually terminates.

Proposition 6 *For any $q \in \{1, 2, \dots, n\}$ and $\alpha \geq 2$, there exists $p \in [\min X_q, \max X_q]$ such that $|I_{p, \varepsilon_q} \cap X_q| < \alpha$.*

Proof We prove this by contradiction. Suppose that there exists $q \in \{1, 2, \dots, d\}$ such that

$$|I_{p, \varepsilon_q} \cap X_q| \geq \alpha$$

for all $p \in [\min X_q, \max X_q]$. Let $m = \min X_q$ and $M = \max X_q$.

For $k = 1, 2, \dots, n$, take

$$p_k = m + 2(k-1)\varepsilon_q.$$

Then we have

$$\bigcap_{k=1}^n I_{p_k, \varepsilon_q} = \bigcap_{k=1}^n [m + (2k-3)\varepsilon_q, m + (2k-1)\varepsilon_q] = \emptyset$$

and

$$\begin{aligned} \bigcup_{k=1}^n I_{p_k, \varepsilon_q} &= \bigcup_{k=1}^n [m + (2k-3)\varepsilon_q, m + (2k-1)\varepsilon_q] \\ &= [m - \varepsilon_q, M + \varepsilon_q] \\ &\supseteq [m, M]. \end{aligned}$$

But $|I_{p_k, \varepsilon_q} \cap X_q| \geq \alpha$ for all $k = 1, 2, \dots, n$ and so X_q has at least αn elements. This is a contradiction since X has n elements. \square

Theorem 7 Fix $q \in \{1, 2, \dots, d\}$ and $\alpha \geq 2$ and let

$$A = \{p \in [m, M] : |I_{(p, \varepsilon_q)} \cap X_q| \geq \alpha\}$$

where $m = \min X_q$ and $M = \max X_q$ such that $m < M$. Then we have

$$\mu_{\text{Bor}}(A) < \frac{l_q}{\alpha}$$

where μ_{Bor} is the Borel measure on \mathbb{R} .

Proof If A is empty, it is trivial. Otherwise, suppose that A is nonempty. Consider a map

$$\begin{aligned} f : \mathbb{R} &\rightarrow \mathbb{Z} \\ p &\mapsto |I_{p, \varepsilon_q} \cap X_q|. \end{aligned}$$

Let $A' = f^{-1}([\alpha, \infty))$ so that $A = A' \cap [m, M]$. For $p \in A'$, put

$$\begin{aligned} m_p &= \min(I_{p, \varepsilon_q} \cap X_q), \\ M_p &= \max(I_{p, \varepsilon_q} \cap X_q). \end{aligned}$$

Since X_q is finite,

$$R = \max\{M_p - m_p : p \in A'\} < 2\varepsilon_q$$

is well-defined. Now let

$$r = \min\{|x - y| \mid x \neq y, x, y \in X_q\}.$$

If $r = 0$, then X_q has n duplicates and thus $m = M$. Since $m < M$, this is impossible. Thus, we have $r > 0$.

Since $A \neq \emptyset$, there exists $p_1 \in A'$. Then we have the half-open interval containing p_1 :

$$B_1 = (a_1, b_1] = (M_{p_1} - \varepsilon_q, m_{p_1} + \varepsilon_q] \subseteq A'.$$

If $B_1 \cup \dots \cup B_{k-1} \subsetneq A'$ with $k \geq 2$, there exists

$$p_k \in \mathbb{R} \setminus (B_1 \cup \dots \cup B_{k-1}) \quad \text{such that} \quad |I_{(p_k, \varepsilon_q)} \cap X_q| \geq \alpha.$$

Similarly, we have the half-open interval containing p_k :

$$B_k = (a_k, b_k] = (M_{p_k} - \varepsilon_q, m_{p_k} + \varepsilon_q] \subseteq A'.$$

Since $B_k \not\subseteq B_{k-1}$, we have

$$B_k \setminus B_{k-1} = \begin{cases} (a_k, b_k] & \text{if } B_k \cap B_{k-1} = \emptyset, \\ (a_k, a_{k-1}] & \text{if } a_{k-1} < b_k < b_{k-1}, \\ (b_{k-1}, b_k] & \text{if } a_{k-1} < a_k < b_{k-1}. \end{cases}$$

Since $a_i = M_{p_i} - \varepsilon_q$, $b_i = m_{p_i} + \varepsilon_q$, we have

$$\begin{aligned} &\mu_{\text{Bor}}(B_k \setminus B_{k-1}) \\ &\geq \min(2\varepsilon_q - (M_{p_k} - m_{p_k}), |M_{p_{k-1}} - M_{p_k}|, |m_{p_k} - m_{p_{k-1}}|) \\ &\geq \min(2\varepsilon_q - R, r). \end{aligned}$$

Therefore,

$$\begin{aligned} &\mu_{\text{Bor}}(B_1 \cup \dots \cup B_k) - \mu_{\text{Bor}}(B_1 \cup \dots \cup B_{k-1}) \\ &= \mu_{\text{Bor}}(B_k \setminus B_{k-1}) \\ &\geq \min(2\varepsilon_q - R, r) \\ &> 0 \end{aligned}$$

where $\min(2\varepsilon_q - R, r)$ is the fixed positive number for all k . Since $m(A') \leq l_q + 2\varepsilon_q < \infty$, the following sequence

$$B_1 \subsetneq (B_1 \cup B_2) \subsetneq \cdots \subsetneq (B_1 \cup \cdots \cup B_k) \subsetneq \cdots \subseteq A'$$

must terminate, that is, $B_1 \cup \cdots \cup B_t = A'$ for some t . In particular, A' is Borel measurable. Note that a union of half-open intervals is also a union of half-open intervals. Then we may assume B_i are mutually disjoint half open intervals of the form $(a_i, b_i]$. For each B_i , take small $r_i > 0$ and put $c_i = \left\lfloor \frac{b_i - a_i - r_i + 2\varepsilon_q}{2\varepsilon_q} \right\rfloor \in \mathbb{Z}$. Then we can take

$$\beta_{i,j} = b_i - 2\varepsilon_q(j-1) \in B_i$$

for $j = 1, 2, \dots, c_i$. Note that $\beta_{i,j} - \beta_{i,j-1} = 2\varepsilon_q$ for $j = 0, 1, 2, \dots, c_i$. Thus the half open intervals $I_{\beta_{i,1}, \varepsilon_q}, \dots, I_{\beta_{i,c_i}, \varepsilon_q}$ of length $2\varepsilon_q$ are mutually disjoint. Since $\beta_{i,j} \in B_i \subseteq A'$ we have $|I_{\beta_{i,j}, \varepsilon_q} \cap X_q| \geq \alpha$ for $j = 1, 2, \dots, c_i$ and

$$\begin{aligned} |B_i \cap X_q| &\geq |I_{\beta_{i,1}, \varepsilon_q} \cap X_q| + \cdots + |I_{\beta_{i,c_i}, \varepsilon_q} \cap X_q| \\ &\geq \alpha c_i \\ &= \left\lfloor \frac{b_i - a_i - r_i + 2\varepsilon_q}{2\varepsilon_q} \right\rfloor \alpha \\ &> \left(\frac{b_i - a_i - r_i}{2\varepsilon_q} \right) \alpha. \end{aligned}$$

Case 1. $m \in A$ and $M \in A$.

For this case $\mu_{\text{Bor}}(A') = \mu_{\text{Bor}}(A) + 2\varepsilon_q$ and

$$\begin{aligned} n &\geq |A' \cap X_q| \\ &= |(B_1 \cup \cdots \cup B_t) \cap X_q| \\ &= |B_1 \cap X_q| + \cdots + |B_t \cap X_q| \\ &> \sum_{i=1}^t \left(\frac{b_i - a_i - r_i}{2\varepsilon_q} \right) \alpha \\ &= \frac{\alpha}{2\varepsilon_q} \mu_{\text{Bor}}(A') - \frac{r_1 + \cdots + r_t}{2\varepsilon_q} \alpha. \end{aligned}$$

Letting $r_1, \dots, r_t \rightarrow 0$, we have

$$n \geq \frac{\alpha}{2\varepsilon_q} \mu_{\text{Bor}}(A')$$

and

$$\begin{aligned} \mu_{\text{Bor}}(A) &= \mu_{\text{Bor}}(A') - 2\varepsilon_q \\ &\leq \frac{2\varepsilon_q}{\alpha} n - 2\varepsilon_q \\ &= \frac{l_q}{\alpha} \frac{n}{n-1} - 2\varepsilon_q \\ &= \frac{l_q}{\alpha} \left(\frac{n-\alpha}{n-1} \right) \\ &< \frac{l_q}{\alpha}. \end{aligned}$$

Case 2. ($m \in A$ and $M \notin A$) or ($m \notin A$ and $M \in A$).

For this case we have $\mu_{\text{Bor}}(A') = \mu_{\text{Bor}}(A) + \varepsilon_q$ and $|A' \cap X_q| \leq n-1$. Similarly, we have

$$n-1 \geq \frac{\alpha}{2\varepsilon_q} \mu_{\text{Bor}}(A').$$

Then

$$\begin{aligned}\mu_{\text{Bor}}(A) &< \mu_{\text{Bor}}(A') \\ &\leq \frac{2\varepsilon_q}{\alpha}(n-1) \\ &= \frac{l_q}{\alpha}.\end{aligned}$$

Case 3. $m \notin A$ and $M \notin A$.

For this case, $|A' \cap X_q| \leq n-2$ and we have

$$n-2 \geq \frac{\alpha}{2\varepsilon_q} \mu_{\text{Bor}}(A').$$

Then

$$\begin{aligned}\mu_{\text{Bor}}(A) &\leq \mu_{\text{Bor}}(A') \\ &\leq \frac{2\varepsilon_q}{\alpha}(n-2) \\ &< \frac{2\varepsilon_q}{\alpha}(n-1) \\ &= \frac{l_q}{\alpha}.\end{aligned}$$

□

Corollary 2 The probability that we repeat **Stage 1** is less than $\frac{1}{\alpha}$.

Proof Notice the following equivalence

$$\text{Repeat } \mathbf{Stage\ 1} \Leftrightarrow |I_{(p, \varepsilon_q)} \cap X_q| \geq \alpha \text{ in } \mathbf{Stage\ 2}.$$

By **Theorem 7**, we have

$$\begin{aligned}&\text{Prob}(|I_{(p, \varepsilon_q)} \cap X_q| \geq \alpha) \\ &= \frac{\mu_{\text{Bor}}(\{p \in [\min X_q, \max X_q] : |I_{(p, \varepsilon_q)} \cap X_q| \geq \alpha\})}{\mu_{\text{Bor}}([\min X_q, \max X_q])} \\ &< \frac{l_q}{\alpha} \frac{1}{l_q} \\ &= \frac{1}{\alpha}.\end{aligned}$$

□

Remark 7

- i) The probability that Algorithm 2 terminates within $N-1$ iterations is *at least* $1 - (\frac{1}{\alpha})^N$ and it is an increasing function with respect to α and N .
- ii) For $\alpha = 2$, $(\frac{1}{2})^6$ is an upper bound of the probability that we repeat **Stage 1** 6 times. Therefore, $1 - (\frac{1}{2})^6 = 0.984375$ refers to a lower bound of the probability that the iteration terminates within 5 trials (Table 3), and this probability further increases for $\alpha \geq 3$. Therefore, we need not concern ourselves with infinite loops.

N	1	2	3	4	5	6
$1 - (\frac{1}{2})^N$	0.50	0.75	0.88	0.94	0.97	0.98

Table 3: Lower bounds for the probability that the iteration terminates within $N - 1$ trials with $\alpha = 2$

Example 3 shows that the upper bound $\frac{l_q}{\alpha}$ in **Theorem 7** is *sharp*.

Example 3 Let $\alpha \geq 2$. Fix an integer k . For each $i = 1, 2, \dots, \alpha$, define

$$L_i = \{(j, i) \mid j = 1, 2, \dots, k\}.$$

Take

$$X = L_1 \cup \dots \cup L_\alpha \cup \{(0, 0), (\alpha k + 1, 0)\} \subseteq \mathbb{R}^2.$$

Then X has $n = \alpha k + 2$ elements. Suppose that the dimension cut is $q = 1$. Note that

$$\varepsilon_1 = \frac{l_1}{2(n-1)} = \frac{\alpha k + 1}{2(\alpha k + 2 - 1)} = \frac{1}{2}.$$

Then every point in $X_1 = \{0, 1, 2, \dots, k, \alpha k + 1\}$ except 0 and $\alpha k + 1$ has α duplicates. Let

$$A = \{p \in [0, \alpha k + 1] : |I_{(p, \varepsilon_1)} \cap X_1| \geq \alpha\}.$$

Then we have $\mu_{\text{Bor}}(A) = k \times 2\varepsilon_1 = k$. On the other hand, by **Theorem 7**, we have an upper bound of $\mu_{\text{Bor}}(A)$:

$$\frac{l_1}{\alpha} = \frac{\alpha k + 1}{\alpha} = k + \frac{1}{\alpha}.$$

Note that

$$k + \frac{1}{\alpha} \rightarrow \mu_{\text{Bor}}(A) \text{ as } \alpha \rightarrow \infty.$$

This shows that the upper bound converges to $\mu_{\text{Bor}}(A)$.

5.4 Convergence and Complexity

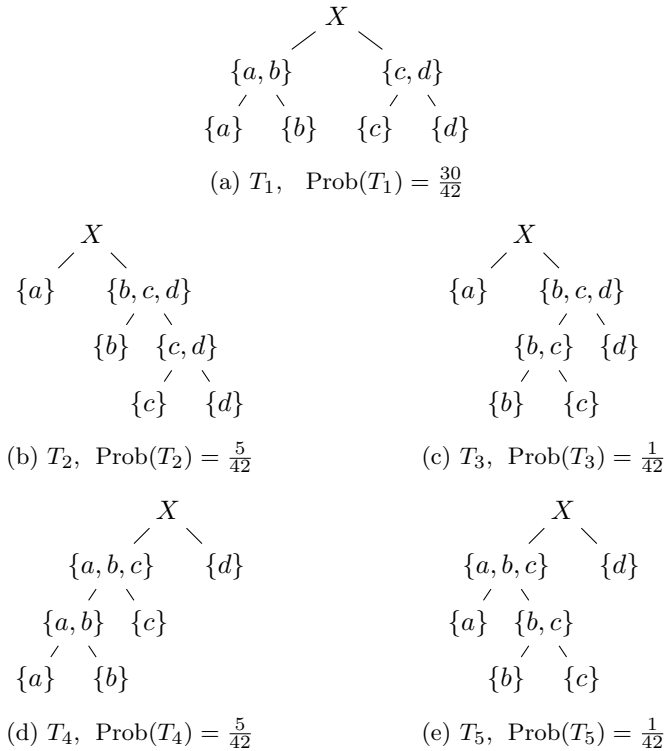
Both the IF and RRCF algorithms have similar time complexities $O(mn \log n)$ where n is the data size and m is the number of trees [13, 15]. The density-aware partitioning affects only the selection of split values, which are repeated. The number of repetitions, denoted as N , does not depend on the data size. In fact, N is bounded above by M where M follows a geometric distribution with parameter $\frac{1}{\alpha}$ (Remark 7). Therefore, the expected number of repetitions is α , which is independent of the data size.

Now, we will observe that the anomaly scores in the WIF and WRCF do not converge to the same limit as in IF and RRCF, respectively, as demonstrated in Example 4.

Example 4 Let $X = \{a, b, c, d\} \subseteq \mathbb{R}^2$ be a set of four points defined as follows:

$$a = (0, 0), \quad b = (1, 0), \quad c = (6, 0), \quad d = (7, 0).$$

Since the y -coordinates of all points in X are zero, we will only consider $P|_{Q=1}$. Table 4 shows the anomaly score of each algorithm. Note that the anomaly scores of

**Fig. 12:** The graphs of T_i with $\text{Prob}(T_i)$ (Example 4)

$x \in X$	a	b	c	d
RRCF	1.31	1.12	1.12	1.31
WRCF	1	1	1	1
IF	0.48	0.45	0.45	0.48
WIF	0.5	0.5	0.5	0.5

Table 4: Anomaly scores for the RRCF, WRCF, IF, and WIF

all points in X with the WIF and WRCF are equal, as Algorithm 2 allows building only tree T_1 in Fig. 12.

Ordinary Partitioning: In both the IF and RRCF algorithms, there are five possible trees denoted as T_i . The $\text{Prob}(T_i)$ represents the probability of obtaining T_i during the tree-building process based on Algorithm 1, as illustrated in Fig. 12.

Density-Aware Partitioning: Choose $\alpha = 2$ in Algorithm 2. Note that the radius ε_1 of X_1 is $\frac{7}{6}$ and so

$$|I_{p, \varepsilon_1} \cap X_1| < 2 \Leftrightarrow p \in \left(\frac{7}{6}, \frac{35}{6} \right]$$

but $(\frac{7}{6}, \frac{35}{6}] \subseteq (1, 6)$. So, we have the tree T_1 (Fig. 12) with the probability $1 - (\frac{1}{3})^{N+1}$, where N is the number of trials we repeat Stage 1 in Algorithm 2. In other words, with the WIF and WRCF algorithms, we always obtain the tree T_1 .

6 Examples

In this section we conduct a comparative analysis of the RRCF and WRCF algorithms across two distinct domains: time series data (6.1) and Euclidean data (6.2). Additionally, we evaluate the IF, WIF, RRCF, and WRCF algorithms using benchmark data sets (6.3).

6.1 Time series Data

6.1.1 Synthetic data

Consider the following time series data $\{X_t\}$ with $t = 1, 2, \dots, 730$,

$$X_t = \begin{cases} 80 & \text{if } t = 235, 234, \dots, 254 \\ 50 \sin(\frac{2\pi}{50}(t - 30)) & \text{elsewhere} \end{cases}.$$

With the shingle, window, and forest sizes of 4, 256, and 40, respectively, the RRCF and WRCF algorithms yield Fig. 13. It shows that both the RRCF and WRCF algorithms detect the desired anomalies at $t = 235$ and 254 successfully. The figure also shows that the WRCF algorithm converges faster than the RRCF (shown in blue ($N = 10$) and orange ($N = 100$) lines).

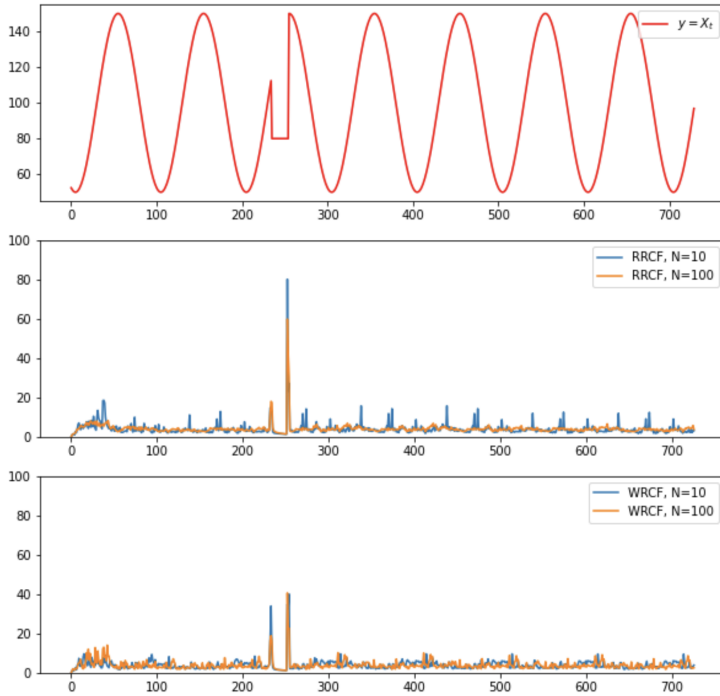


Fig. 13: X_t and Avg-CODISP of RRCF and WRCF

6.1.2 GDP growth rate data

Gross Domestic Product (GDP) is a monetary measure of the market value of all final goods and services produced in a specific period. The GDP growth rate for each period is defined as the ratio of the difference between GDP values from the current period to the next period to the GDP value from the earlier period, multiplied by 100.

$$\text{GDP Growth Rate} = \left(\frac{\text{GDP}_{\text{current period}} - \text{GDP}_{\text{earlier period}}}{\text{GDP}_{\text{earlier period}}} \right) \times 100$$

When economic shocks, such as the global oil shock (1980) and the global financial crisis (2009), hit the world, the GDP of each country plunged. We apply the RRCF and WRCF algorithms to the GDP growth rate data of Korea [21] with the following parameters: shingle size = 2, window size = 8, and the number of iterations = N . The results are shown in Fig. 14. The top figure displays the anomalies detected where **CODISP** > 3 with both the RRCF and WRCF algorithms. The middle and bottom figures show the **Avg-CODISP**s of the RRCF (middle) and WRCF (bottom) for $N = 10$ (blue) and $N = 100$ (orange). As shown in those figures, the WRCF algorithm yields faster convergence than the RRCF.

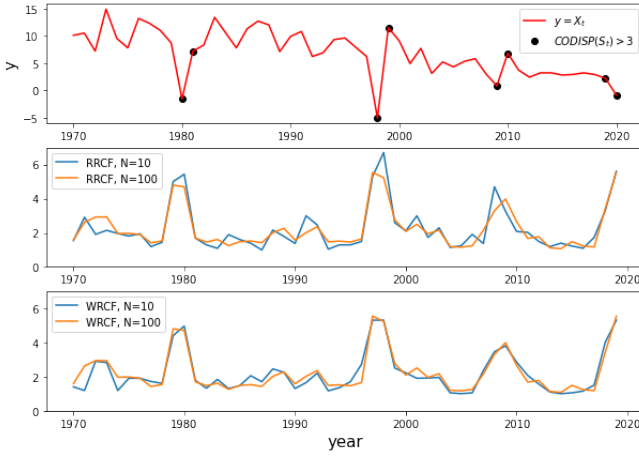


Fig. 14: Korea GDP versus year (top) and **Avg-CODISPs** of RRCF (middle) and WRCF (bottom)

Year	Event	RRCF	WRCF
1980	Oil Shock	4.4	4.4
1981	Oil Shock Recovery	4.5	5
1998	IMF Credit Crisis	5.4	5.3
1999	IMF Credit Crisis Recovery	5.3	5.3
2009	Global Finance Crisis	3.4	3.5
2010	Global Finance Crisis Recovery	3.9	3.8
2019	COVID-19	3.7	4
2020	COVID-19	5.6	5.3

Table 5: Economic shocks in Korea and **CODISPs** of RRCF and WRCF

Table 5 shows the CODISPs of the RRCF and WRCF with $N = 100$. As seen in the table, both algorithms yield similar CODIPS values and capture all the desired economic shocks in the data.

6.1.3 NewYork Taxi data

We also use the taxi ridership data from the NYC Taxi Commission [22], where the total number of passengers is aggregated over a 30-minute time window [15]. We employ the following parameters: shingle size = 48 (a day), sample size = 1000, and total iteration number = N . The deleting and inserting method (Section 3.4) is used.

The top figure of Fig. 15 displays the given taxi ridership data, and the subsequent figures depict the graphs of **Avg-CODISPs** with the RRCF (red) and WRCF (blue) algorithms for $N = 10, 50, 500$. The top figure shows the taxi ridership data, with special days (such as holidays) highlighted in green, during

which the anomalous behaviors of taxi ridership occurred. We consider **Avg-CODISP**s with $N = 500$ as the limit values for both algorithms, regarding days with **Avg-CODISP** > 14 as anomalies for both algorithms. The bottom two figures show a total of 17 anomalies identified at the limit ($N = 500$), highlighted with orange lines in each **Avg-CODISP** figure as a reference. We consider these 17 limit anomalies as the *desired* anomalies that we are looking for. Any other anomalies detected are considered *false* anomalies. The actual meaning of those anomalies in the physical sense is not of interest; we are mainly concerned with the convergent behaviors of each method.

To assess how each method detects the desired anomalies as N changes, we computed **Avg-CODISP** with $N = 10$ and $N = 50$. As shown in the second figure, the RRCF algorithm identified 8 anomalies out of the 17 desired anomalies. However, the third figure shows that the WRCF found all 17 anomalies. Thus, the WRCF algorithm seems to identify all the desired anomalies faster than the RRCF algorithm. Figures with $N = 10$ also reveal that the WRCF found more false anomalies than the RRCF. Figures with $N = 50$ show that the RRCF algorithm found more desired anomalies than with $N = 10$, but not all 17, while the WRCF algorithm still identified all 17 desired anomalies and found fewer false anomalies than with $N = 10$. This experiment also implies that the WRCF algorithm provides faster convergent results than the RRCF algorithm.

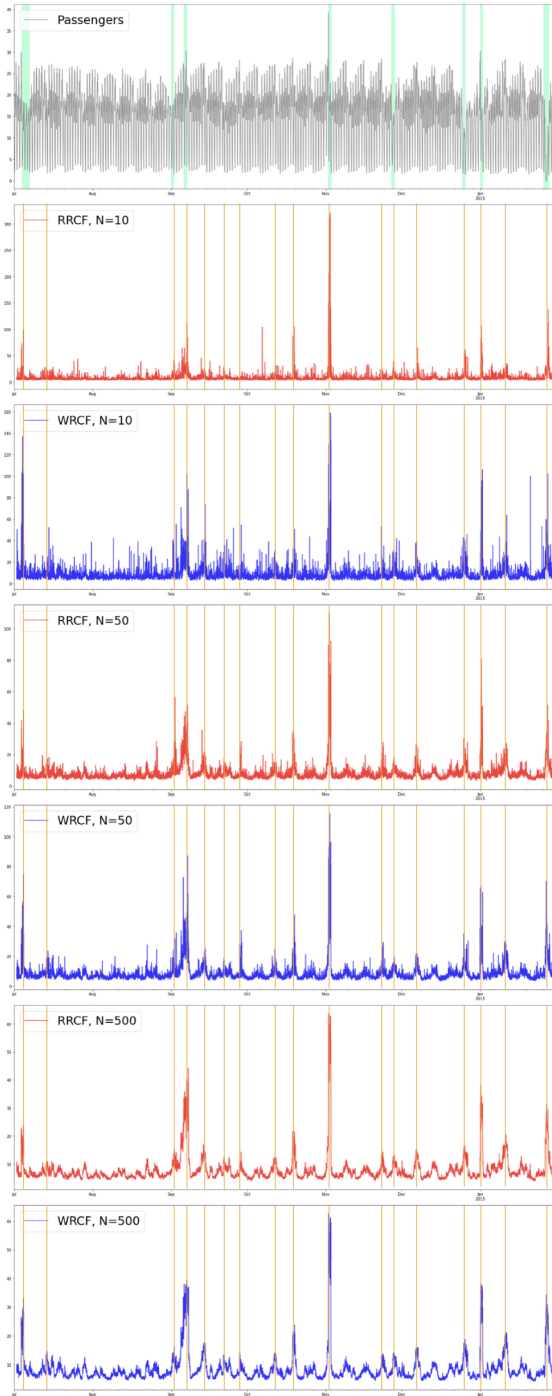


Fig. 15: Avg-CODISPs of RRCF (red) and WRCF (blue)

6.2 Euclidean Data

6.2.1 10 points with one cluster

Suppose we have the following data set $X = \{a, b, c, d, e, f, g, h, i, j\} \subseteq \mathbb{R}^2$, depicted in Fig. 16, where

$$\begin{aligned} a &= (-23.6, -2), & b &= (-12.1, 0.3), & c &= (0, 1.7), \\ d &= (-1.1, 1.2), & e &= (0.6, 1), & f &= (0.3, -0.3), \\ g &= (0.1, -0.7), & h &= (1.3, -0.8), & i &= (-0.7, -0.7), & j &= (-0.6, 0.1). \end{aligned}$$

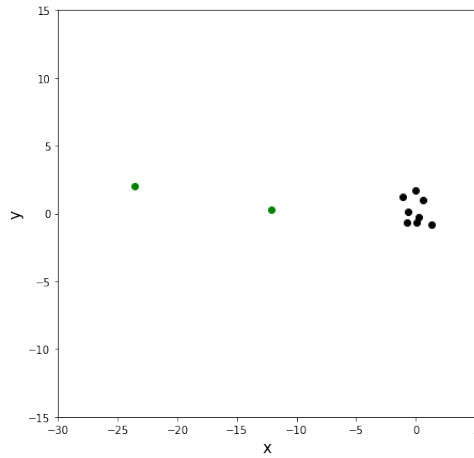


Fig. 16: The graph of X , $\mu(X) = 0.55$

Tables 6 and 7 show **Avg-CODISP** of each point $x \in X$ where N is the number of iterations.

N	a	b	c	d	e	f	g	h	i	j
1	4	4	2	1.6	1	2	1	4	3	1
2	6.5	6	1.8	1.8	1.3	1.5	1	3	2.3	1.6
3	7.3	6.6	1.8	2.2	1.2	1.3	1	3	1.9	1.7
4	7.8	2	3.4	1.2	1.3	1.3	1	3.3	1.7	1.9
5	8	7.2	2.8	3.1	1.1	1.2	1	4	1.5	1.9
10	7.5	6.5	2.1	3.1	1.1	1.2	1	4	1.5	1.9
10000	6.1	5.2	2.5	2.3	1.6	1.4	1.2	3.3	1.7	2.0

Table 6: RRCF: **Avg-CODISP**s for each point

N	a	b	c	d	e	f	g	h	i	j
1	9	8	7	6	2	1	1	5	2	4
2	9	8	4.2	4	3	1	1	6	2	2.7
3	7.3	6.7	3.8	3	2.3	1	1	5	2	2
4	7.8	7	4.6	2.8	2	1.2	1.2	4.4	1.8	2.5
5	7	6.4	4.1	2.6	1.8	1.1	1.1	4.9	1.6	3.2
10	6	5.7	3.2	2.1	1.8	1.3	1.1	3.8	1.8	2.4
10000	6.4	5.8	2.7	2.4	1.7	1.4	1.2	3.4	1.6	2.0

Table 7: WRCF: **Avg-CODISP**s for each point

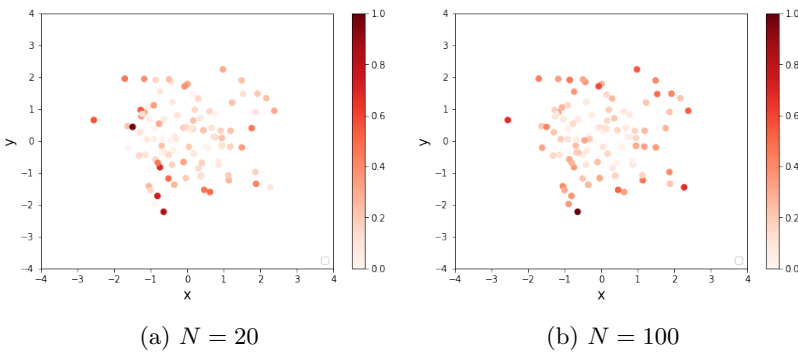
Note that points a, b have higher CODISP values than the others in both algorithms. The values

$$\sum_{x \in X} (|\mathbf{Avg-CODISP}(x, 10000) - \mathbf{Avg-CODISP}(x, 10)|)$$

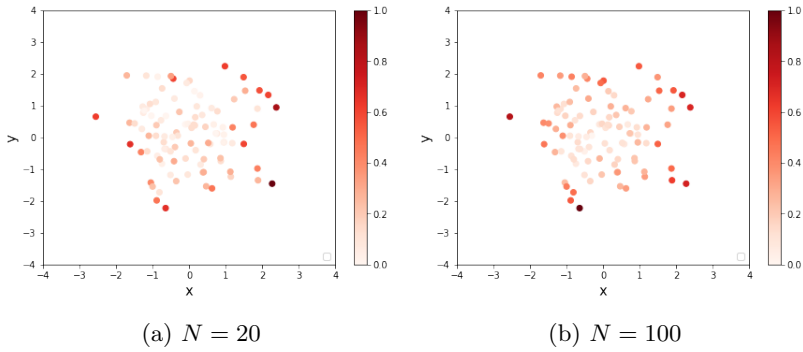
of Tables 6 and 7 are 5.9 and 2.6, respectively. This shows that the WRCF algorithm converges to $\mathbf{Avg-CODISP}(x, 10000)$ faster than the RRCF.

6.2.2 Normally distributed points

Let \mathbb{X} be a set of 100 points in \mathbb{R}^2 where each $(x, y) \in \mathbb{X}$ is obtained from the random variable (X, Y) such that both X and Y are normally distributed. The density measure $\mu(X)$ is 0.06. One could assume that the likelihood of a point being an anomaly increases as its distance from the origin $(0, 0)$ grows. We run the RRCF and WRCF algorithms with the sample size $= 10$ and the number of iterations $= N$.

**Fig. 17:** **Avg-CODISP** of RRCF

The color bars in Figs. 17 and 18 depict the (normalized) **Avg-CODISP** values for the points in X . When $N = 100$, both the RRCF and WRCF

**Fig. 18: Avg-CODISP of WRCF**

algorithms capture those points far from the origin as anomalies. When $N = 20$, the RRCF algorithm does not capture anomalies well compared to the WRCF algorithm since many points far from the origin have lower **CODISP** values with the RRCF. To capture anomalies well enough, the RRCF needs a larger value of N than the WRCF.

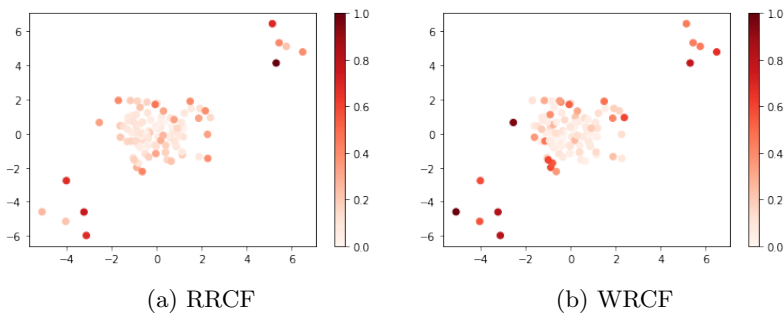
6.2.3 Normally distributed points with anomaly clusters

Let X_1, X'_2 and X'_3 be sets of 100, 5 and 5 points in \mathbb{R}^2 , respectively, where each point in the sets is obtained from the random variable (X, Y) such that both X and Y are normally distributed. Denote

$$X_2 = X'_2 - (5, 5) = \{(x, y) - (5, 5) \mid (x, y) \in X'_2\},$$

$$X_3 = X'_3 + (5, 5) = \{(x, y) + (5, 5) \mid (x, y) \in X'_3\}$$

and set $X = X_1 \cup X_2 \cup X_3$. The density measure $\mu(X)$ is 0.07. It may be presumed that X_2 and X_3 are clusters of anomalies.

**Fig. 19: Avg-CODISP of RRCF and WRCF**

The color bars in Fig. 19 refer to the normalized **Avg-CODISP**s for the points in X . If we consider points with (normalized) **Avg-CODISP** > 0.5 as anomalies, the RRCF captures 3 points in X_2 and 4 points in X_3 as anomalies but the WRCF captures all the points in X_2 and X_3 as anomalies. Moreover, the WRCF captures points that are far from the origin in X_1 as anomalies whereas the RRCF treats the whole X_1 as normal data.

6.2.4 Normally distributed clusters with noises

Let X_1 be a set of two clusters where each cluster is obtained by multiplying 0.1 by normally distributed 100 points with translation. Let X_2 be a set of normally distributed 40 points. Let $X = X_1 \cup X_2$. In Fig. 20, the blue dots

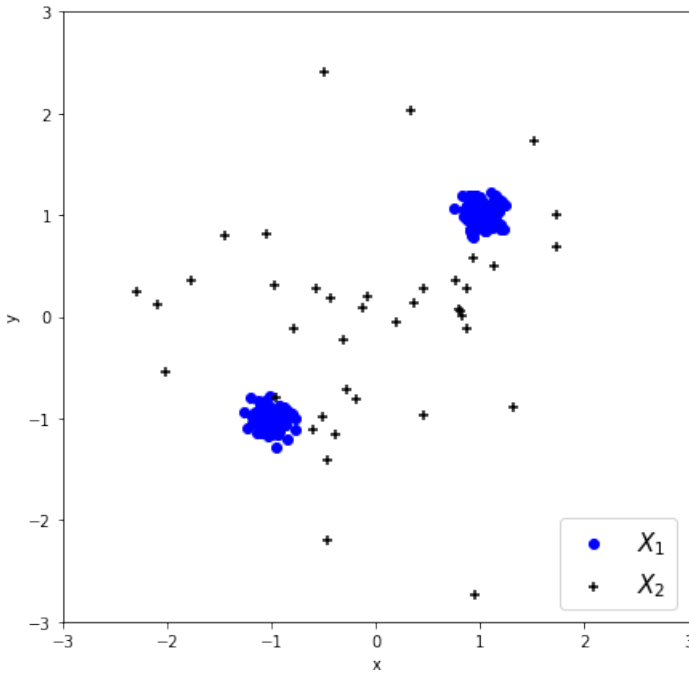


Fig. 20: The graph of X , $\mu(X) = 0.09$

denote the data set of X_1 and the black crosses of X_2 . As shown in the figure, X_1 is composed of two clusters while the elements of X_2 are not clustered but scattered. Thus apparently X_2 seems more like noise or anomalies compared to the clustered X_1 . We apply the RRCF and WRCF algorithms with the sample size = 20 and the number of iterations = N . In Figs. 21 and 22, the more red a point is, the higher **Avg-CODISP** it has. Note that the RRCF algorithm cannot capture 3 points near $(-2, 0)$ as anomalies with $N = 10$ and

they are regarded as anomalies with $N = 100$. However, the WRCF captures the 3 points as anomalies even with $N = 10$.

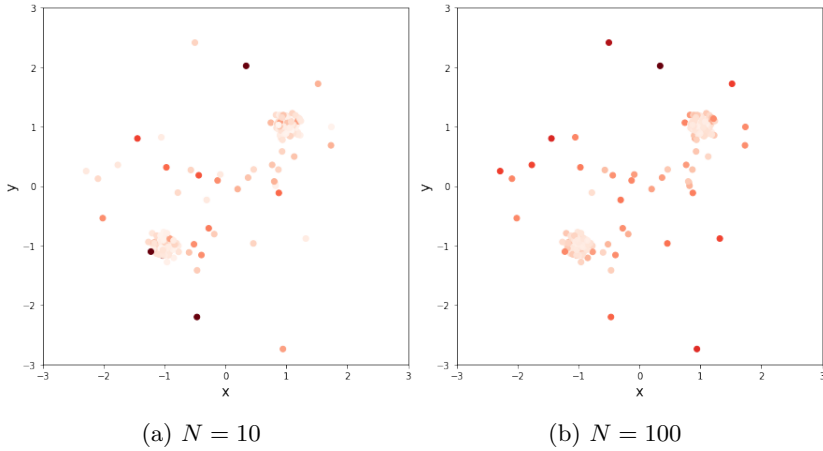


Fig. 21: Avg-CODISP of RRCF

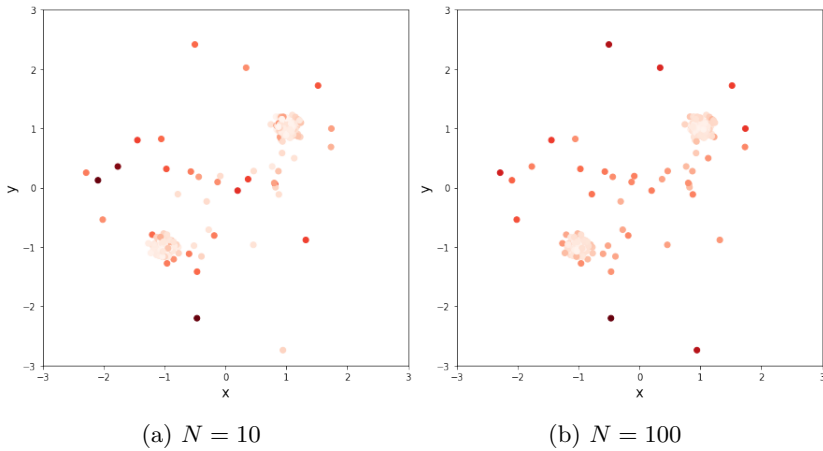
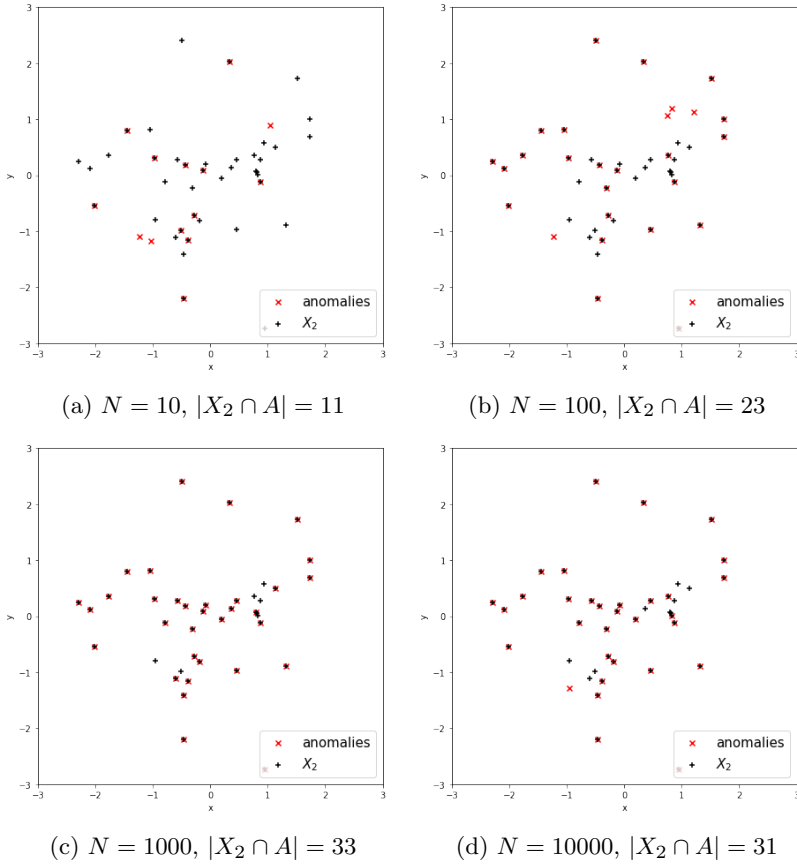
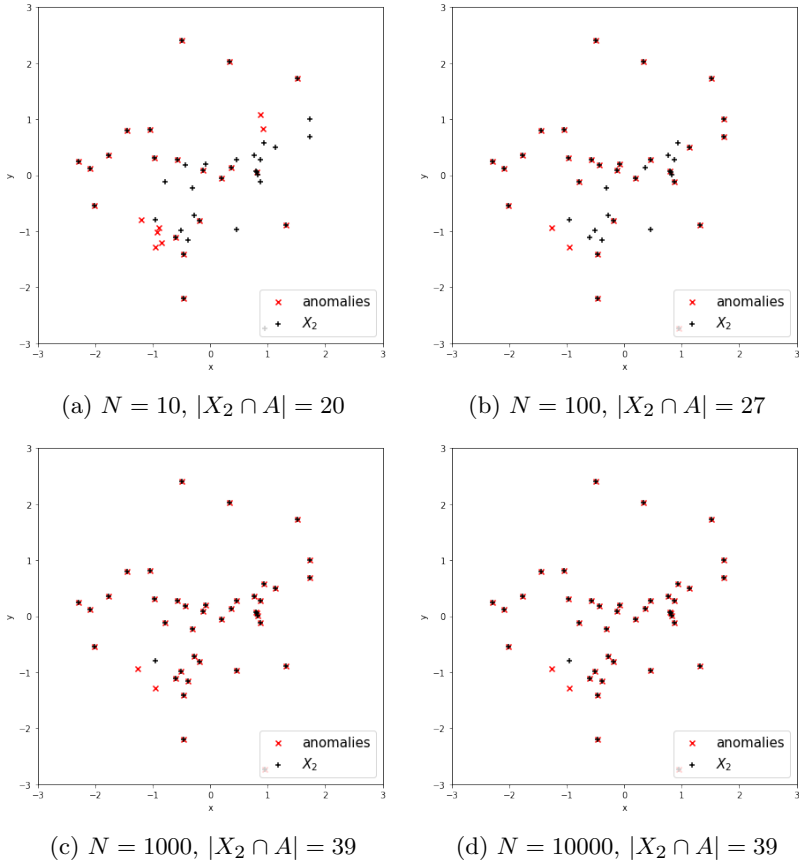


Fig. 22: Avg-CODISP of WRCF

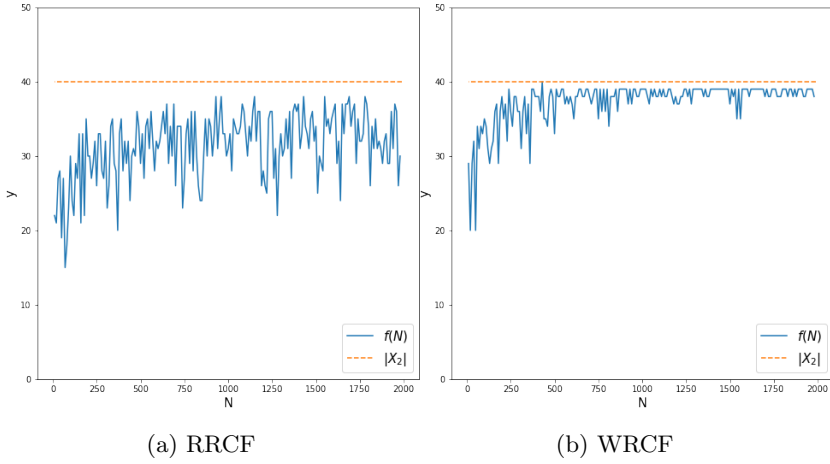
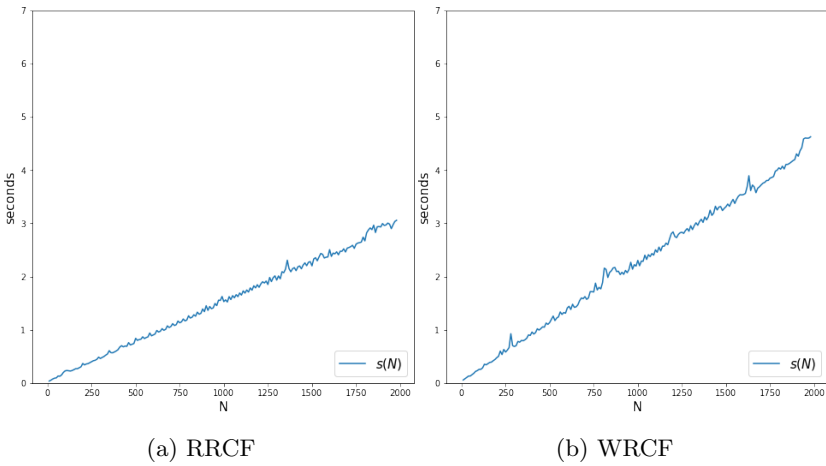
Let A be the subset of X whose points have the normalized Avg-CODISP > 0.35 . One may think that A is the set of detected anomalies whereas X_2 is the set of anomalies. One may think that $|X_2 \cap A|$, which is the number of detected anomalies in X_2 , measures how well the algorithm detects anomalies. In Figs. 23 and 24, we observe that, for every value of N used, the WRCF consistently exhibits a larger $|X_2 \cap A|$ compared to the RRCF.

**Fig. 23:** Detected anomalies of RRCF

In order to understand qualitatively how the number of the detected anomalies behaves with N , we let $f(N) = |X_2 \cap A|$, the number of the detected anomalies. Note that the desired number of anomalies in X is $|X_2| = 40$. Figure 25 shows the graph of $f(N)$ versus N with the RRCF (left) and WRCF (right) algorithms where $N = 10, 20, 30, \dots, 2000$. In the figure, the orange dotted line indicates the desired number of anomalies, i.e., $|X_2| = 40$. The number of the detected anomalies, $f(N)$, is depicted in blue. As shown in Fig. 25, $f(N)$ of the RRCF fluctuates highly more than the WRCF. For the WRCF, the magnitude of the fluctuation decreases with N while the magnitude of the fluctuation with the RRCF does not change even though N increases. According to the pattern of $f(N)$ of the RRCF (left), it seems that $f(N)$ does not necessarily reach the desired number of anomalies even though N is highly large. We clearly see that the WRCF is more effective and stable than the RRCF as N increases. $f(N)$ with the WRCF reaches the desired number of $|X_2| = 40$ much faster than the RRCF.

**Fig. 24:** Detected anomalies of WRCF

To check the computational complexity of both algorithms for this problem, we let $s(N)$ be the running time of each algorithm in seconds. Figure 26 shows the running time $s(N)$ versus N of the RRCF (left) and WRCF (right) algorithms. First of all, as expected, we observe that $s(N)$ is linear with respect to N for both algorithms. The WRCF has a slightly steeper slope of $s(N)$ than the RRCF – the slope of $s(N)$ of the WRCF is about 1.5 times larger than that of the RRCF. When N is small, the difference is not significant.

**Fig. 25:** $y = f(N)$ **Fig. 26:** $y = s(N)$

6.3 Benchmark data sets

The performance of the IF, WIF, RRCF, and WRCF algorithms is evaluated across eight benchmark datasets. The details of every dataset used in the experiments are outlined in Table 8. The AUC score, commonly used to evaluate the performance of a binary classification model, is measured on the y -axis, while the x -axis represents the tree size for each dataset in Table 8.

Figures 27 and 28 show the results for each data set. The AUC scores are represented by the blue, orange, green and red colors for the IF, WIF, RRCF and WRCF, respectively. As the AUC score approaches 1, the algorithm

demonstrates higher accuracy in binary classification. The results indicate that the WIF outperforms the IF, and the WRCF surpasses the RRCF across all evaluated data sets.

Data set	Instances	Features	Description
Http [23]	567,498	3	The original data contains 41 attributes. However, it is reduced to 3 attributes, focusing on ‘http’ service.
Ionosphere [24]	351	33	Binary classification of radar returns from the ionosphere.
Breastw [25]	683	9	Binary classification of breast cancer.
Cover [26]	286,048	10	Classification of 7 forest cover types based on attributes such as elevation, aspect, and more.
Satellite [27]	6,435	36	Multi-spectral values of pixels in 3x3 neighbourhoods in a satellite image, and the classification associated with the central pixel in each neighbourhood.
Thyroid [28]	3,772	6	Classification data set for ANNs.
MNIST [29]	7,603	100	Handwritten digits data set transformed for outlier detection, treating digit-zero as inliers and digit-six as outliers.
Musk [30]	3,062	166	Binary classification of Musk data set.

Table 8: Benchmark data sets

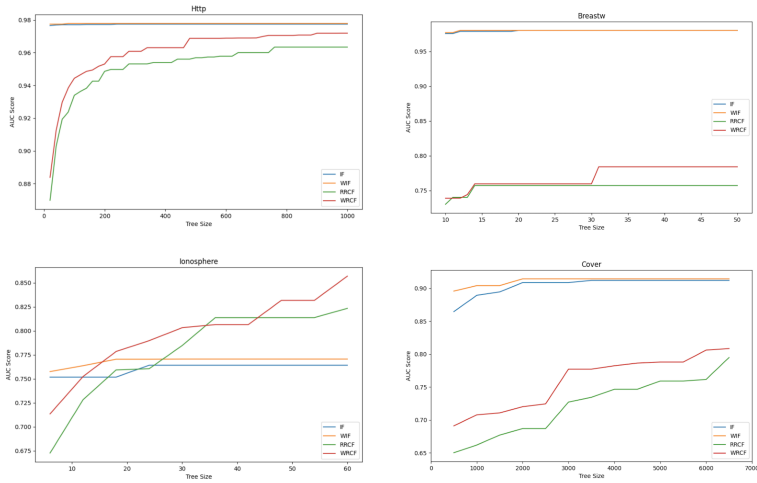


Fig. 27: AUC scores versus tree size for Http and Inosphere (left column) and Breastw and Cover (right column) data sets

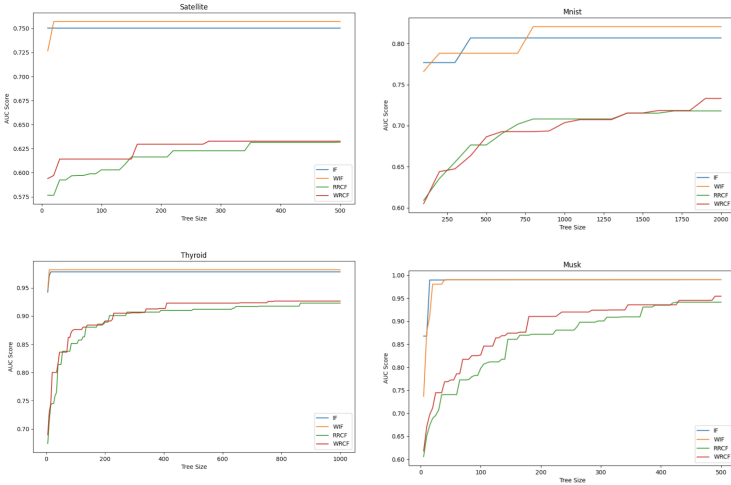


Fig. 28: AUC scores versus tree size for Http and Inosphere (left column) and Breastw and Cover (right column) data sets for Satellite and Thyroid (left column) and MNIST and Musk (right column) data sets

7 Conclusion

The IF and RCF algorithms are efficient for anomaly detection. The RRCF algorithm, a variant of RCF, is efficient as it selects the dimension cuts based on the shape of data. In this paper, we showed that the IF and RRCF can be further improved using the density-aware partitioning when choosing the split values and proposed new algorithms, which we refer to as the weighted IF (WIF) and weighted RCF (WRCF) methods. With the density-aware partitioning, the data structure is adaptively considered and faster convergence is obtained in determining the anomaly scores. To construct the WIF and WRCF, we proposed the concept of the density measure. We provided various mathematical properties of the density measure and density-aware partitioning. Numerical results provided in this paper verify that the proposed WIF and WRCF algorithms perform better than the IF and RRCF algorithms, respectively, especially when the data has non-uniformity in its structure.

References

- [1] Bartos, M.D., Mullapudi, A., Troutman, S.C.: rrcf: Implementation of the robust random cut forest algorithm for anomaly detection on streams. *Journal of Open Source Software* **4**(35), 1336 (2019). <https://doi.org/10.21105/joss.01336>
- [2] Goldstein, D., et al.: Automated transient identification in the dark energy survey. *The Astronomical Journal* **150**(3), 82 (2015). <https://doi.org/10.1088/0004-6256/150/3/82>
- [3] Goldstein, M., Uchida, S.: A comparative evaluation of unsupervised anomaly detection algorithms for multivariate data. *PLOS ONE* **11**(4), 1–31 (2016). <https://doi.org/10.1371/journal.pone.0152173>
- [4] Ruff, L., Vandermeulen, R.A., Görnitz, N., Binder, A., Müller, E., Müller, K.-R., Kloft, M.: Deep semi-supervised anomaly detection. In: *International Conference on Learning Representations*
- [5] Gao, F., Li, J., Cheng, R., Zhou, Y., Ye, Y.: Connet: Deep semi-supervised anomaly detection based on sparse positive samples. *IEEE Access* **9**, 67249–67258 (2021). <https://doi.org/10.1109/ACCESS.2021.3077014>
- [6] Peterson, L.E.: K-nearest neighbor. *Scholarpedia* **4**(2), 1883 (2009)
- [7] Patrick, E.A., Fischer III, F.P.: A generalized k-nearest neighbor rule. *Information and control* **16**(2), 128–152 (1970)
- [8] Dudani, S.A.: The distance-weighted k-nearest-neighbor rule. *IEEE Transactions on Systems, Man, and Cybernetics* (4), 325–327 (1976)

- [9] Gates, G.: The reduced nearest neighbor rule (corresp.). IEEE transactions on information theory **18**(3), 431–433 (1972)
- [10] Breunig, M.M., Kriegel, H.-P., Ng, R.T., Sander, J.: Lof: identifying density-based local outliers. In: Proceedings of the 2000 ACM SIGMOD International Conference on Management of Data, pp. 93–104 (2000)
- [11] Kriegel, H.-P., Kröger, P., Schubert, E., Zimek, A.: Loop: local outlier probabilities. In: Proceedings of the 18th ACM Conference on Information and Knowledge Management, pp. 1649–1652 (2009)
- [12] He, Z., Xu, X., Deng, S.: Discovering cluster-based local outliers. Pattern recognition letters **24**(9-10), 1641–1650 (2003)
- [13] Liu, F.T., Ting, K.M., Zhou, Z.-H.: Isolation forest. In: 2008 Eighth IEEE International Conference on Data Mining, pp. 413–422 (2008). <https://doi.org/10.1109/ICDM.2008.17>
- [14] Hariri, S., Carrasco Kind, M., Brunner, R.J.: Extended isolation forest. IEEE Transactions on Knowledge and Data Engineering, 1–1 (2019). <https://doi.org/10.1109/TKDE.2019.2947676>
- [15] Guha, S., Mishra, N., Roy, G., Schrijvers, O.: Robust random cut forest based anomaly detection on streams, 2712–2721 (2016). PMLR
- [16] Bartos, M.D., Mullapudi, A., Troutman, S.C.: rrcf: Implementation of the robust random cut forest algorithm for anomaly detection on streams. Journal of Open Source Software **4**(35), 1336 (2019)
- [17] Knuth, D.E.: The Art of Computer Programming, Volume 3: (2nd Ed.) Sorting and Searching. Addison Wesley Longman Publishing Co., Inc., USA (1998)
- [18] Breiman, L.: Bagging predictors. Machine learning **24**(2), 123–140 (1996)
- [19] Chu, C.-S.J.: Time series segmentation: A sliding window approach. Information Sciences **85**(1), 147–173 (1995). [https://doi.org/10.1016/0020-0255\(95\)00021-G](https://doi.org/10.1016/0020-0255(95)00021-G)
- [20] Folland, G.B.: Real Analysis: Modern Techniques and Their Applications, (2013)
- [21] ECOS - Economic Statistics System. [https://ecos.bok.or.kr/#/Statistic sByTheme/KoreanStat100](https://ecos.bok.or.kr/#/Statistic%20ByTheme/KoreanStat100). Accessed: January 10, 2024
- [22] NYC Taxi & Limousine Commission - Trip Record Data. http://www.nyc.gov/html/tlc/html/about/trip_record_data.shtml. Accessed: January 10, 2024

- [23] Stolfo, S., Fan, W., Lee, W., Prodromidis, A., Chan, P.: Kdd cup 1999 data (1999). DOI: <https://doi.org/10.24432/C51C7N>
- [24] Sigillito, V., Wing, S., Hutton, L., Baker, K.: Ionosphere (1989). DOI: <https://doi.org/10.24432/C5W01B>
- [25] Wolberg, W.: Breast Cancer Wisconsin (Original) (1992). DOI: <https://doi.org/10.24432/C5HP4Z>
- [26] Blackard, J.: Covertype (1998). DOI: <https://doi.org/10.24432/C50K5N>
- [27] Srinivasan, A.: Statlog (Landsat Satellite) (1993). DOI: <https://doi.org/10.24432/C55887>
- [28] Quinlan, R.: Thyroid Disease (1987). DOI: <https://doi.org/10.24432/C5D010>
- [29] Deng, L.: The mnist database of handwritten digit images for machine learning research. *IEEE Signal Processing Magazine* **29**(6), 141–142 (2012)
- [30] Chapman, D., Jain, A.: Musk (Version 2) (1994). DOI: <https://doi.org/10.24432/C51608>